Environmental Fluid Mechanics (2021) 21:521–559
https://doi.org/10.1007/s10652-021-09790-w

REVIEW ARTICLE

Cooling tower plume abatement and plume modeling: a review

Shuo Li[1] · **M. R. Flynn**[1]

Received: 20 September 2020 / Accepted: 8 April 2021 / Published online: 15 April 2021

Abstract
Visible plumes above wet cooling towers are of great concern due to the associated aesthetic and environmental impacts. The parallel path wet/dry cooling tower is one of the most commonly used approaches for plume abatement, however, the associated capital cost is usually high due to the addition of the dry coils. Recently, passive technologies, which make use of free solar energy or the latent heat of the hot, moist air rising through the cooling tower fill, have been proposed to minimize or abate the visible plume and/or conserve water. In this review, we contrast established versus novel technologies and give a perspective on the relative merits and demerits of each. Of course, no assessment of the severity of a visible plume can be made without first understanding its atmospheric trajectory. To this end, numerous attempts, being either theoretical or numerical or experimental, have been proposed to predict plume behavior in atmospheres that are either uniform versus density-stratified or still versus windy (whether highly-turbulent or not). Problems of particular interests are plume rise/deflection, condensation and drift deposition, the latter consideration being a concern of public health due to the possible transport and spread of Legionella bacteria.

Keywords Cooling tower · Visible plume · Crosswind · Ambient turbulence · Drift deposition

1 Introduction

Cooling towers are heat dissipation devices commonly found in industrial plants and HVAC systems. In general, two types of cooling towers, i.e. wet and dry, are used; these exploit evaporative and non-evaporative heat transfer mechanisms, respectively. As shown in Figs. 1 and 2, wet cooling towers are classified as counterflow and crossflow according to the respective directions of the air and water streams. As defined by Holiday and Alsayed [54], sustainability in a cooling system encompasses efficient operation, impact on the environment, depletion of natural resources and ecology. For instance, a reduction in the fan power consumption or pump head facilitates a more efficient operation. On the

✉ Shuo Li
shuo10@ualberta.ca

[1] Department of Mechanical Engineering, University of Alberta, Edmonton, AB T6G 1H9, Canada

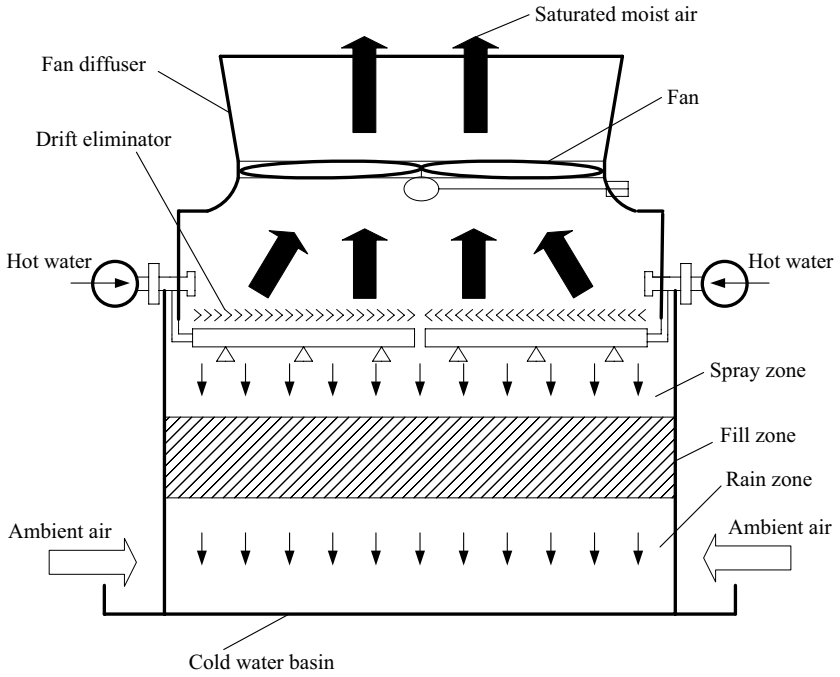

Fig. 1 Schematic of a counterflow wet cooling tower. The thick white and black arrows denote the incoming ambient air into the cooling tower and the hot, humid air coming out of the wet section, respectively. The thin arrows denote the water stream.

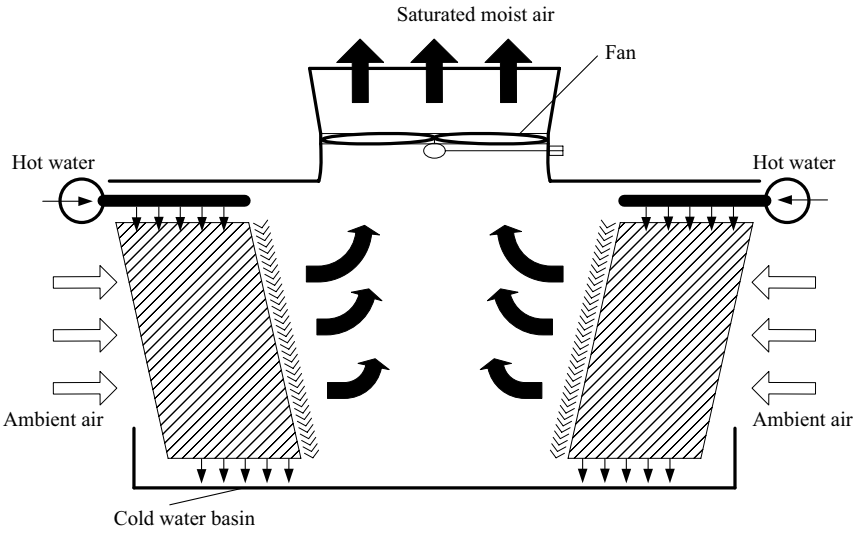

Fig. 2 Schematic of a crossflow wet cooling tower. Arrow types are as in Fig. 1. Note that the fill is installed at an angle to the vertical to account for the inward motion of water droplets due to the drag associate with the incoming air [81].

other hand, visible plumes, water conservation and drift deposition are closely related to the environmental impact, as is plume rise, which dictates the maximum ground concentration of air pollutants.

Modeling the heat and mass transfer in a wet cooling tower, particularly within the fill zone, has been performed since the seminal work of Merkel [100], followed by the effectiveness-NTU method [63], Poppe method [116] and Klimanek method [73]. A comprehensive comparison between the Merkel, effectiveness-NTU and Poppe methods is presented in Kloppers and Kröger [76, 77], which concluded that the Poppe method, being the most algebraically-involved, is also the most accurate for the design of hybrid wet/dry cooling towers. Meanwhile, the Klimanek method is largely equivalent to the Poppe method (cf. Table 1 of Klimanek and Białecki [73]) except that its governing equations consider as the independent variable elevation within the tower rather than the water temperature. In the Merkel method, the cooling tower exit air is always assumed to be exactly saturated, which is inaccurate in case of extreme (hot dry or cold humid) conditions. The Poppe and Klimanek methods, on the other hand, avoid this deficiency and thus improve the prediction of the water evaporation rate.

The water lost due to evaporation, drift and blowdown[1] in a typical wet cooling tower is 3% to 5% of the circulating water [53]. To compensate this loss, make-up water, where available, is required, this to avoid an accumulation of impurities and contaminants. The source and chemistry of this make-up water have an obvious impact on the difficulty of maintaining water quality. Also, although blowdown ensures that a portion of the recirculating water is discharged and replenished with pure make-up water, the challenges associated with contaminant concentration increases is not restricted to engineering equipment/process: water quality adversely affects the discharged air quality due to e.g. drift contained in the moist air exiting the tower. The situation is especially significant when considering Legionella bacteria, which may be carried by the drift. Talbot [138] revealed the acute effects of salt drift on vegetation from a closed-cycle salt water cooling tower, but the damage was limited to the close proximity of the tower. A review by Walser et al. [147] summarized the severe health problems of legionellosis outbreaks due to the operation of cooling towers. Even when Legionella bacteria are eradicated by appropriate chemical treatments, a visible plume may be considered as a nuisance for the fact that it is perceived as aesthetically-unpleasant and it has the potential to cause reduced visibility and/or icing on neighboring surfaces (e.g. roadways) when the ambient temperature is sufficiently low. Latimer and Samuelsen [85] conducted a theoretical examination of the visual impact of a cooling tower plume focusing on the effects of plume coloration and reduced visual range. This work was followed up many years later by Lee [89] who performed an environmental impact assessment of cooling towers in a nuclear power plant. Notably, Lee [89] quantified the effects of visible plumes in terms of plume length and shadowing (and the commensurate loss of solar energy), fogging and icing, and salt and water depositing. Moreover, these effects were tested by Lee [89] under different cooling tower configurations, heat load per tower and air flow rate per tower.

In the context of plume abatement, reference is often made to the standard plume performance testing code—CTI ACT 150 [9]. The 150 code proposes two levels of plume guarantee for hybrid wet/dry cooling towers, Level 1 and Level 2. Level 1 specifies that the measured exhaust relative humidity should be lower than the guarantee relative humidity, determination of which comes from the plume characteristic performance

[1] Blowdown is the water discharged from the system to control the concentrations of salts and other impurities in the circulating water.

curves provided by the cooling tower manufacturer. However, Level 1 does not require complete mixing of the wet and dry airstreams within the plenum chamber (defined as the enclosed space above the drift eliminator and below the fan in an induced draft tower). Level 2, on the other hand, is more stringent than Level 1, i.e. it requires satisfaction of a mixing criteria. The principle of this mixing criteria is to check whether all measured exhaust air properties are within an acceptable variation compared to the average properties. The measured parameters of key interest are the relative humidity and air velocity. To achieve complete mixing, mixing devices are commonly added to the plenum chamber as a result of which fan power consumption increases. Notwithstanding the distinction between Level 1 and Level 2, recent studies, e.g. Li et al. [91], indicate that visible plumes can be partially or completely eliminated even with partial mixing within the plenum chamber. Using the approach of Li et al. [91], fewer internal mixing devices are required and the moist air discharged to the environment is "shielded" by a sheath of buoyant but much drier air in the manner of Houx Jr et al. [57].

The previous discussion focuses principally on heat and mass transfer processes internal to a cooling tower. Having set the stage, we turn for the reminder of this section to exterior processes, i.e. plumes in the atmosphere. Cooling tower plumes are similar to, but different than, chimney stack plumes. One obvious distinction is the presence of large amounts of water vapor in the cooling tower case. Nonetheless, only a moderate amount of water vapor will condense contributing, in the process, to an increase of plume buoyancy. Thus simple analytical formulas like the MTT model [110] and Briggs' "two-thirds" law, gives reasonable estimates for cooling tower plume rise [17]. To improve model performance, more sophisticated theoretical models have been proposed to predict the plume trajectory and dilution simultaneously. These integral-type theoretical models are efficient and useful tools, but are limited to boundary layer type flows in unbounded environments. Some phenomena are beyond on the reach of these models, e.g. recirculation, which occurs when a strong wind blows over a line of cooling tower cells, leading to a one-sided increase in the wet-bulb temperature for the incoming air. To resolve these more complex flow interactions, guidance is sought from CFD simulation and/or similitude laboratory experiment. A similar appeal must be made when examining the details of plume bifurcation or the complicated manifestations of plume rise through a turbulent environment.

The main goals of this review are two-fold: (1) to summarize the strategies for plume abatement and to describe some of the physics that underlies these strategies, (2) to give a selective description of plume modeling approaches that are necessary to better understand plume abatement strategies. These two goals serve to improve efforts to design and construct cooling towers that are more sustainable and less energy intensive. Our focus is restricted to mechanical draft cooling towers (see e.g. Figs. 1 and 2) but the general principles related, more especially, to atmospheric dispersion of plumes, apply also to natural draft cooling towers.

The rest of the review is organized as follows. Section 2 discusses the frequency and severity of plume visibility. Section 3 describes various plume abatement approaches. Section 4 focuses on plume modeling with emphasis on theoretical, CFD and laboratory experimental approaches. Special topics such as plume rise in a turbulent environment, plume bifurcation and drift deposition are discussed in Sects. 4.4, 4.5 and 4.6, respectively. Finally in Sect. 5 we draw conclusions and outline knowledge gaps/areas for future research.

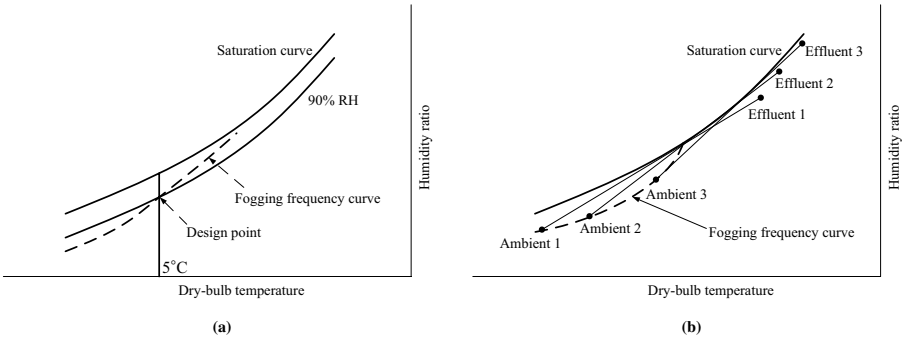

Fig. 3 **a** A fogging frequency curve from Winter [156]. Similar curves can be found in figure 15 of Lindahl and Jameson [93] or figure 2 of Lindahl and Mortensen [94]. **b** Method of generating the fogging frequency curve

2 Plume visibility

Winter [156] reviewed the influence of increasing public awareness of visible plumes on cooling tower selection for combined cycle gas turbine power stations in the UK. He suggested that fogging frequency should be used to evaluate plume abated towers; this can be calculated by making reference to a fogging frequency curve on a psychrometric chart as shown in Fig. 3a. According to the 150 code [9], and for a given operating condition, the fogging frequency curve is defined as a curve that divides the psychrometric chart according to whether a visible versus invisible plume is expected. Illustrated in Fig. 3b is the method for generating such a curve; this method references the collection of ambient conditions (for a given operating condition) that allow the fan to ambient mix-lines to be exactly tangent to the saturation curve. Given site-specific weather statistics, it is possible to determine the fogging frequency at a given location, which can be expressed as the proportion of operating hours wherein visible plumes may occur. The 150 code argues that a typical plume abatement design point should allow 15% to 20% visible plume occurrence based on full year day-night weather statistics. Although theoretically any point on the fogging frequency curve can be chosen as the design point, a design point above the freezing point is recommended in order to test the cooling tower. For example, and in Fig. 3a, the plume abatement design point corresponds to an ambient temperature of 5 °C and relative humidity (RH) of 90%.

Tyagi et al. [144] proposed the so-called plume potential to quantify the visible plume intensity, which is defined as the area between the fan to ambient mix-line and the saturation curve on a psychrometric chart—see Fig. 4. The area in question is evaluated from

$$A = 2 \int_{\omega_2}^{\omega_1} \sqrt{\omega}\, \mathrm{d}\omega, \tag{1}$$

where ω is the humidity ratio in g/kg dry air. Intense fog is anticipated when the area computed by 1 is comparatively large. More recently, and rather than examining intersected areas in a psychrometric chart, Cizek and Nozicka [27] considered the overall volume of the visible plume, which is expressed as an empirical coefficient times the third power of the cooling tower diameter. Cizek and Nozicka [27] revealed that the overall visible plume

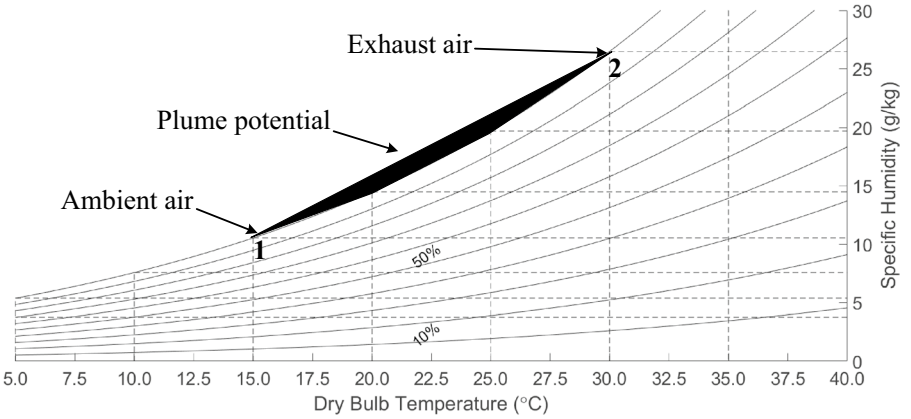

Fig. 4 Visible plume potential defined in Tyagi et al. [144]

volume depends sensitively on the cooling tower diameter, the temperature and humidity of the exhaust and ambient air, but does not depend on the plume source velocity.

3 Visible plume abatement

Veldhuizen and Ledbetter [145] presented a summary of approaches to fog control: (1) preventing fog formation by superheating the plume and altering the cooling method, (2) removing the fog by sedimentation after particle growth by impaction of water droplets on cold surfaces, by chemical desiccation or by electrostatic sweeping (or related air-cleaning methods) of droplet-nucleating particles, and, (3) restricting the fog from reaching ground level by elevating the plume through mechanical jetting or heating. Veldhuizen and Ledbetter [145] pointed out that the difficulty in fog control is the large flow rate of air containing small water droplets.

A more comprehensive review of plume abatement technologies was conducted [94]—see Table 1. The main comparisons are made between parallel path wet/dry (PPWD) cooling towers and more novel approaches such as condensing module technology. PPWD is a traditional plume abatement cooling tower design whereby parallel streams of air flow through the dry and wet sections and then mix in a plenum chamber before being discharged by the fan. Lindahl and Mortensen [94] argued that condensing module technology offers a means to reduce capital and operating costs, and is especially suitable for large back-to-back towers.[2] The physical principles underlining condensing module technology are detailed in Sect. 3.5.

Following the framework outlined in Table 1, the rest of this section is structured as follows. Section 3.1 discusses the method of superheating the exhaust air, which generally occurs in series path wet/dry (SPWD) cooling towers wherein the dry section is added to

[2] The back-to-back tower configuration combines two lines of cooling tower cells into one line, which has a common wall located at the centerplane of the "dual row" towers. The advantage of the back-to-back tower configuration is its reduced footprint compared to an equal number of cooling tower cells arranged in two parallel lines.

Table 1 The evolution of plume abatement designs as summarized in Lindahl and Mortensen [94]

Timeline	Tower design	Advantages	Disadvantages
1960's	Series path wet/dry (SPWD) towers	Well-mixed exhaust air	Full-time pressure drop, widely spaced fins and high pump head for hot water coils
1970's	Parallel path wet/dry (PPWD) towers	Face dampers added to the dry and wet sections, water conserving compared to wet cooling towers	Additional pressure drop due to mixing devices typically used in PPWD counterflow towers
2000's	Condensing module technology	No dry section, high water conservation capability, no mixing devices, low drift rate, less blowdown and make-up through recovery of the near condensate quality water, no pumping head above the wet section, suitable for back-to-back tower configurations	Full-time pressure drop due to its series air path, increased pressure drop due to the air ducts and air-to-air heat exchangers in the plenum chamber

desaturate the air stream before or after it flows through the wet section. Sections 3.2, 3.3 and 3.4 focus on different mixing techniques in the context of PPWD towers. Section 3.5 reviews various water conservation approaches and some novel tower designs.

3.1 Superheating the exhaust air

In a SPWD cooling tower, sensibly heating the exhaust air not only decreases its relative humidity, but also increases its temperature and therefore buoyancy. Research in this category mainly focuses on the heat sources and the associated control strategies for plume abatement. For instance, Wang and Tyagi [149] and Tyagi et al. [144] used heat pumps to heat the exhaust air from wet cooling towers. The advantage is that the coefficient of performance for a heat pump is much greater than unity. However, the inclusion of heat pumps obviously adds to the capital, operational and maintenance costs associated with the cooling tower proper. Later Wang et al. [148] compared three arrangements of heat pump system for plume abatement in a large chiller plant in a subtropical region. Specifically, the evaporative side of the heat pump can be located at the inlet or outlet side of the cooling towers to decrease the cooling water temperature, or alternatively at the evaporative side of the chillers to reduce the return chilled water temperature—see their figures 1 and 3. Meanwhile, the hot water in the dry coils of the hybrid wet/dry cooling tower are provided by heat pumps. Their study indicated that the aforementioned three arrangements have almost identical plume control performance. Regarding the overall energy efficiency, the latter arrangement had much better performance than the former two arrangements. More generally, heat pumps have the thermodynamic advantage of offering combined heating and cooling.

As exhibited schematically in Fig. 5, Wang et al. [150] investigated the application of a solar collector to mitigate the visible plume from wet cooling towers as a case study in Hong Kong. Their discussion revealed that water cooled collectors were more cost-effective than air cooled collectors. They also argued that there should be some alternate heat sources to assist due to the intermittency of solar energy during the day and its complete absence at night.

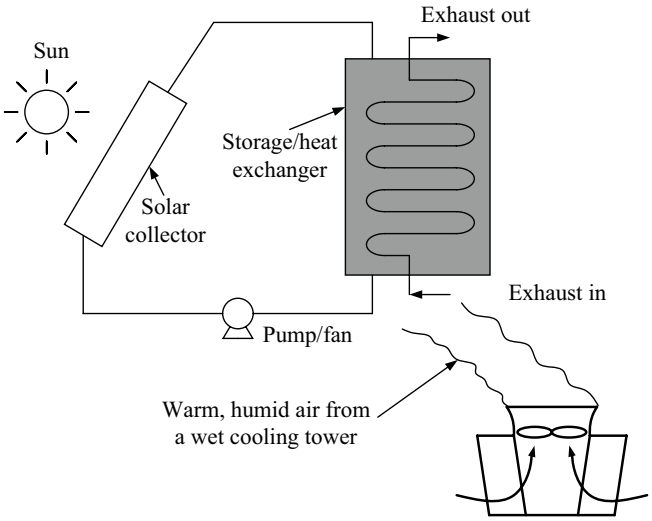

Fig. 5 A water/air cooled flat plate solar collector to heat the exhaust from wet cooling towers

3.2 Enhanced mixing by static devices

Whereas the discussion of Sect. 3.1 focused primarily on small-scale cooling towers e.g. those that form part of air-conditioning systems for commercial buildings, here we return to the larger models more typically found in industry. In a PPWD counterflow cooling tower, the warm, dry air from the dry section and the hot, humid air from the wet section are mixed in the plenum chamber thus reducing the possibility of condensation upon discharge. As expected, a visible plume may occur if the mixing is inadequate. Because the mixing length is relatively short (no more than the height of the plenum plus the fan diffuser), mixing devices are commonly added to promote the mixing between those two (initially) perpendicular air streams. Streng [135] noted that "the optimal shape and arrangement of static mixers as a function of the specific cooling tower geometry is of particular significance".

Generally, deflecting surfaces are used to channelize the flow of dry air and to thereby promote the penetration of at least some fraction of this dry air into the central region of the plenum chamber. Thus the area of contact between the wet and dry air streams greatly increases. Meanwhile, the deflecting structure, if not streamlined in the direction of the wet airstream, tends to generate flow separation and turbulent mixing ensues downstream. Unavoidably, the structural expense can be heavy as can the increased pressure drop. Nonetheless, deflecting surfaces are particularly effective for back-to-back cooling towers where it is difficult to convey adequate dry air to the central wall.

Kinney Jr et al. [71] argued that the geometric orientations of the dry and wet sections impose restrictions on the air flow patterns such that the warm, dry air from the dry section tends to follow a path directly to the nearest lower edges of the fan diffuser. The hot, humid air from the wet section, on the other hand, occupies the central part of the plenum chamber. For enhanced mixing, they proposed that simple flat plates, extending from the lower part of the dry section to the central core of the plenum chamber, are adequate for mixing the two air streams in certain instances.

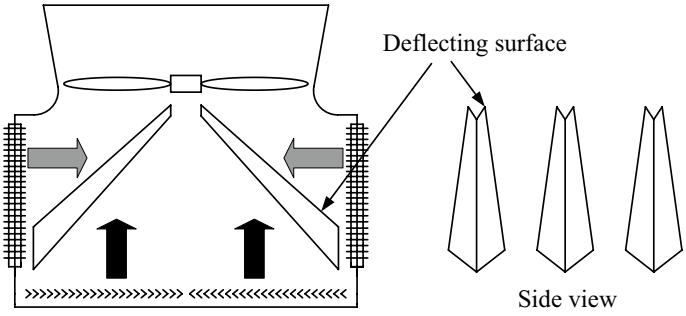

Fig. 6 The tapered V-shaped deflecting surface proposed by Carbonaro [21]

Carbonaro [21] introduced a type of rectilinear deflecting surface (referred to as an air channeling device) with a decreasing V-shaped cross section—see Fig. 6. As compared to e.g. a flat plate, this V-shaped structure along which the dry air travels is expected to impose less obstruction to the upward moving wet air. Moreover, the tapered V-shape cross section can cause some fraction of the dry air flow to overlow and thereby mix into the wet air all along the length of the channel. Schulze [129] proposed the use of truncated pyramid-like mixing baffles inside the plenum chamber. These baffles project transversely into the ascending wet air and direct the dry air into the central region of the plenum chamber. Finally, Ruscheweyh [123, 124] introduced a delta-shaped vortex generator, which facilitates enhanced mixing at the cost of moderate pressure drop. The performance of this type of vortex generator was tested using reduced-scale laboratory experiments that employed smoke for purposes of flow visualization. Without the benefit of the vortex generator, the "wet air" accumulates in the central core upon discharge due to the poor mixing. By contrast, a relatively uniform smoke plume results from the enhanced mixing caused by addition of the vortex generators.

3.3 Enhanced mixing by stirring devices

Moon [107] put a number of circularly spaced guide vanes below the cooling tower fan to induce vortex mixing. In Moon's design, the guide vanes surround a central cylinder that is attached to the axis of rotation of the fan, thus forming a stirring device to blend the dry and wet air—see Fig. 7. The guide vanes are similar to the devices proposed in a much earlier patent by Fernandes [44], who invented a so-called vortex cooling tower. This vortex cooling tower creates a tornado-like motion within the tower and results in low pressure in order to induce flow through the air inlet. The fan illustrated in Fig. 7 may be put to other secondary uses, e.g. a rotary dehumidifier in the absence of the dry section [48].

3.4 Coaxial plume mixing

Houx Jr et al. [57] designed a type of hybrid wet/dry cooling tower with good resistance to recirculation and almost complete elimination of visible plumes. In their design, the dry and wet airstreams are in a coaxial configuration with the former enveloping an inner core of the latter. It should be emphasized that their tower has a large dry cooling section and a small backup wet section. Therefore, this type of tower is categorized as water conserving

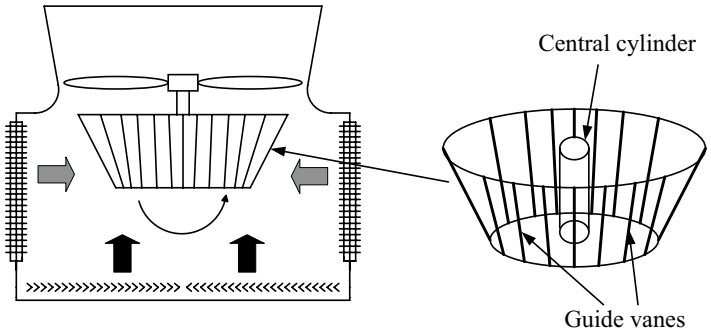

Fig. 7 The stirring vortex mixing device proposed by Moon [107]

(see Sect. 3.5) as compared to a more traditional plume abatement cooling tower in which the cooling load is mainly undertaken by the wet section.

Lindahl and Jameson [93] argued that in crossflow PPWD cooling towers, the saturated wet air leaves the wet section at a velocity twice that of the dry air leaving the dry section. Thus the slower moving dry air tends to surround the faster moving wet air, which naturally results in a coaxial wet/dry plume structure above the cooling tower. They argued that at conditions where a uniform plume would, in theory, be exactly invisible,[3] the aforementioned coaxial plumes continue to mix to become invisible within two to three fan stack diameters. Unfortunately, the coaxial plume structure does not occur naturally in counterflow PPWD cooling towers where the wet and dry airstreams have approximately the same velocity.

Koo [79, 80] proposed a hybrid cooling tower which facilitates mixing resulting in a coaxial structure. Figure 8 shows that the external dry air is sucked into the space between the fan stack and the outer shroud. Thereafter, the dry air is mixed with the wet air discharged by the fan. To increase the mixing efficiency, the inner shroud is made corrugated to induce streamwise vorticity that enhances the mixing between the two airstreams (cf. [146]). This type of lobed mixer can also be put below the fan or at other strategic locations within the plenum chamber to augment mixing. One possible extension associated with a coaxial plume structure is the replacement of the dry coils with solar collectors, which are similar to those used in a solar chimney system (cf. [161]).

Another possible advantage of the coaxial plume structure is that the onset of condensation may be delayed compared to the conventional uniform plume structure [91]. For a uniform plume (unsaturated at the source) under adverse ambient conditions, the fan to ambient mix-line starts in the unsaturated region then crosses the saturation curve and reaches the supersaturation region—see e.g. Fig. 4. In fact, and according to Monjoie and Libert [106], the visible plume occurs immediately at the fan exit, not some elevation above the stack exit. This is because mixing first occurs at the plume boundary upon discharge. Considering a coaxial plume structure, the mixing initially occurs at the ambient/dry air and dry/wet air boundaries, thus both mix-lines are below the saturation curves. As a result, a visible plume is at least abated near the fan stack exit. On the other hand, forcing the dry

[3] The fan to ambient mix-line is exactly tangent to the saturation curve on a psychrometric chart, see Fig. 3b.

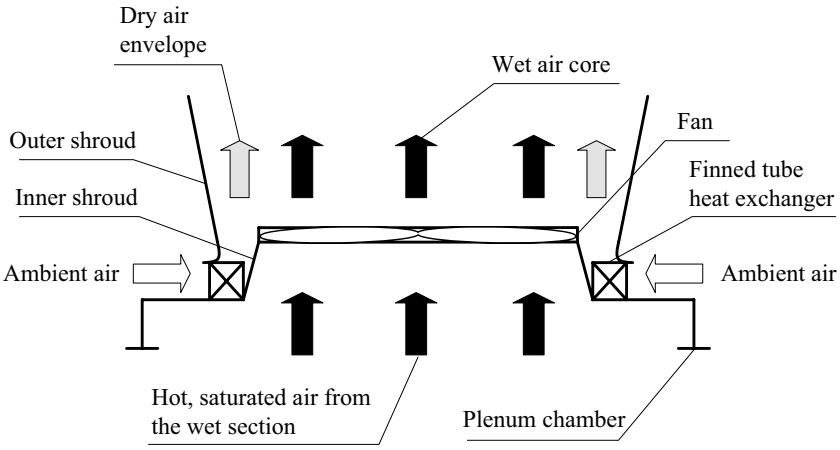

Fig. 8 The plume abatement cooling tower illustrated in Koo [79, 80]. (Figure taken from [91])

air envelope with a much higher velocity yields a jet-like air curtain. Such a curtain has been proposed to effectively enhance plume rise in the presence of wind [145], albeit at the cost of increased fan power. Further details concerning plume modeling are presented in Sect. 4.

3.5 Water conservation and recovery

Even though plume abatement does not necessarily guarantee water conservation, water conservation achieves plume abatement as a side effect. In addition to the previously-discussed model due to Houx Jr et al. [57] from Sect. 3.4, water-conserving towers may be designed in a variety of ways. For instance, Palmer [114] used a cover above the cooling tower to trap the water vapor then channel it back to the cold water basin. As this water vapor flows downwards, it is cooled by the ambient air. Condensation follows and the resulting liquid water can be recycled. A drawback of the cooling tower in question is that it requires additional internal components e.g. air channels and extra fans. These additional components are needed to drive the saturated air.

Mantelli [99] proposed a passive water vapor recovery technology that consists of thermosyphons and porous media as illustrated in Fig. 9. The basic idea is to locate the cooled porous media just downstream of the drift eliminator in a crossflow tower so as to condense and recover the water vapor from the hot, humid air exiting the fill. Meanwhile, the (mostly latent) heat is transferred to the ambient by the condenser part of the thermosyphon. Even without optimization, their device showed the ability to recover 10% of the water that would otherwise be lost to the atmosphere in the form of water vapor.

Another relatively new and commercially-successful technology is the condensing module technology, which incorporates the patented air-to-air (Air2Air^{TM} hereafter) heat exchanger designed by Hubbard et al. [58]. The condensing module is located above the drift eliminator in a counterflow tower, transferring heat from the hot, humid air to the inflowing ambient air through which process water vapor is condensed—see Fig. 10a. The corresponding psychrometric process is illustrated in Fig. 10b. The condensed water can be replaced back into the cold water basin or can be used as a source of purified water thus

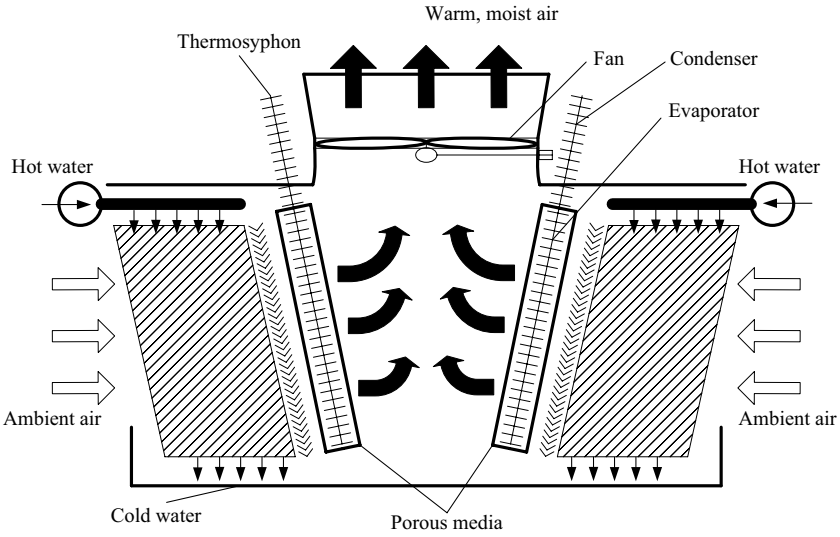

Fig. 9 Schematic of the passive vapor recovery technology consisting of a thermosyphon and porous media in a crossflow cooling tower [99]. The hot, humid air discharged from the drift eliminator is cooled by the evaporator section of the thermosyphon and the working fluid in the evaporator evaporates and rises to the upper condenser section. Thereafter, the working fluid is cooled by the ambient, and condenses and returns to the lower evaporator Sect.

saving the cost associated with maintaining and improving the water quality. Compared to a conventional PPWD cooling tower, the Air2Air^{TM} technology significantly reduces blowdown, and avoids the piping and pumping of hot water to the dry section. Although additional fan power is required to increase the static pressure to pull the air streams through the compact Air2Air^{TM}, the increased power consumption is approximately equal to the counterpart power consumed by a PPWD tower that uses two pass (dry) coils with a siphon loop to reduce pump head [58]. Mortensen [108] reported the capability of the first Air2Air^{TM} water conservation cooling tower at a power plant located in New Mexico. Tests showed that the evaporated water recovery rate was typically 10% to 25% depending on the local climate. Moreover, the Air2Air^{TM} technology achieved effective plume abatement without mixing baffles. This technology has been found to work well even in cold or freezing weather operations [94].

Recently Wang et al. [151] evaluated the plume abatement and water conservation performances of the Air2Air^{TM} heat exchanger. They found that water savings increased significantly under ambient conditions of low temperature and high RH. By choosing several typical months for reference and specifying certain operating parameters (see their Table 4), they revealed that the amount of condensed water was 1.105 kg/s. Assuming the cooling tower operates 7200 h per year, the annual water savings by using Air2Air^{TM} can therefore exceed 2.8×10^7 kg.

A summary of the different plume abatement methods described in Sect. 3 is given in Table 2.

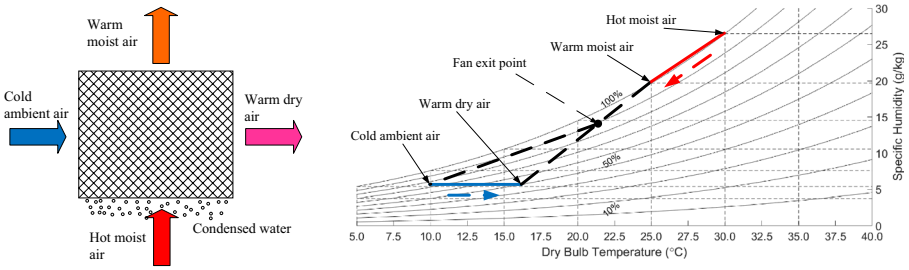

Fig. 10 [Color] **a** Schematic of an Air2Air^{TM} heat exchanger [108]. **b** Psychrometric processes of Air2Air^{TM} technology for plume abatement

4 Plume modeling

4.1 Analytical models

The analytical modeling of moist plumes dates back to the seminal work of Morton [109], which describes a vertically ascending thermal plume in a stationary ambient on the basis of the MTT model. In Morton's formulation, the potential temperature[4] and density, which are conserved during adiabatic mixing processes, are used in the governing equations. G. I. Taylor's entrainment hypothesis [139], which relates the entrainment velocity to the mean vertical velocity of the plume, is the closure condition. Importantly, Morton's analysis assumes a still atmosphere, but this restriction is relaxed in subsequent work that includes wind forcing. To this end, Slawson and Csanady [133] summarize the three distinct stages in the evolution of a plume subject to wind forcing where, in each case, a different entrainment assumption must be adopted. Specifically, mixing in the initial, intermediate and final stages is respectively governed by the plume's self-generated turbulence, environmental turbulence in the inertial subrange and energy containing eddies. The MTT model is only valid in the initial phase wherein the plume's own turbulence is dominant. The bent-over assumption, which states that the plume becomes quasi-horizontal rapidly upon discharge, was adapted by Slawson and Csanady [133] to formulate a modified set of plume rise equations.

On the basis of the work by Morton [109] and Slawson and Csanady [133], Csanady [34] studied bent-over moist plumes and found that an initially saturated plume will begin to re-evaporate upon release, provided that the ambient is unsaturated and the excess temperature of the plume is below a given threshold. Meanwhile, he argued that the influence of condensation and evaporation on the plume trajectory is minor. The subsequent study of bent-over plumes of Wigley and Slawson [153] indicated that condensation always occurs close to the plume source. Slawson and Csanady [134] examined the effect of atmospheric stability[5] on plume rise. Wigley and Slawson [154] compared the behavior of wet

[4] The potential temperature, θ, of an air parcel is the temperature the parcel would have if it were brought adiabatically to the standard pressure. In symbols, we write $\theta = T\left(\frac{P_0}{P}\right)^{R/c_{pa}}$, where T is the thermodynamic temperature at pressure P, P_0 is the standard pressure, R is the gas constant of air and c_{pa} is the heat capacity of air at constant pressure.

[5] The stability of atmosphere is parameterized by the buoyancy frequency, $N = \sqrt{-\frac{g}{\rho_a}\frac{\mathrm{d}\rho_a}{\mathrm{d}z}} \simeq \sqrt{\frac{g}{\theta_a}\frac{\mathrm{d}\theta_a}{\mathrm{d}z}}$, which is the natural frequency of oscillation of a fluid parcel if disturbed from its equilibrium position. The atmosphere can be either stable ($N^2 > 0$), neutral ($N^2 = 0$) or unstable ($N^2 < 0$).

Table 2 Summary of the different plume abatement methods described in Sect. 3

Method/mechanism	Additional source/equipment	Preferred tower configuration or weather condition
Superheating the exhaust air	Heat pump [144, 148, 149] and solar collectors [150]	HVAC cooling towers, suitable for high relative humidity
Enhanced mixing using static and non-static mixers	Deflecting surfaces [21, 71, 129], vortex generators [123, 124] and stirring mixing devices [107]	Cooling towers (including back-to-back towers) with Level 2 plume abatement criterion [9]
Coaxial plume mixing	Hybrid (crossflow) towers [57, 79, 80, 93]	Cooling towers designed with Level 1 plume abatement criterion [9]
Cooling the hot, humid air	Water vapor channel [114], thermosyphon system [99], air-to-air heat exchangers [58, 94, 151]	Preferred in large back-to-back towers and in arid regions; good functionality even in freezing weather conditions

(condensed) and dry (uncondensed) plumes under different atmospheric conditions. Later Wigley [152] included the dynamics of droplet growth in the condensation phase.

These early attempts to model plume rise and condensation typically apply two key assumptions. The former is the bent-over assumption. The latter is an entrainment assumption (for the initial phase), $v_e = \beta\,|w|$, where v_e is the entrainment velocity, w is the vertical component of the mean streamwise velocity of the plume and β is an empirical entrainment coefficient—see Fig. 11. For the case of nontrivial ambient turbulence, three different entrainment assumptions are summarized in Table 2 of Briggs [16]—see Sect. 4.4. Briggs [17] presented a comprehensive review of plume modeling under various ambient conditions, and a detailed formulation of the relevant conservation equations was given. As a starting point, it is appropriate to discuss Briggs's "two-thirds" law of plume rise. Then step by step, we review the improvements upon this simplest analytical model and outline the more sophisticated plume models that have been derived since the publication of Briggs's seminal work.

4.1.1 Foundational theoretical models

The classic Briggs's formula [15] for bent-over buoyant plume rise in a neutral crossflow reads

$$z = 1.6\,F_b^{1/3}\,U_a^{-1}\,x^{2/3}, \tag{2}$$

where z is the height of the plume centerline above the stack exit, U_a is the mean horizontal wind velocity and x is the horizontal distance downstream of the plume source. The source specific buoyancy flux is $F_b = g\frac{\rho_a-\rho_0}{\rho_a}U_0\,r_0^2$, in $\mathrm{m}^4/\mathrm{s}^3$, where $\rho_a = \rho_a(z)$ is the density of ambient air, ρ_0 is the plume source density and r_0 is the actual plume source radius. Briggs's equation was later revised to include the effects of finite source radius and source momentum [17, 37]:

$$z = \left[\frac{3}{2\,\beta^2}\left(\frac{F_b}{U_a^3}\,x^2 + 2\frac{F_m}{U_a^2}\,x\right) + \left(\frac{R_0}{\beta}\right)^3\right]^{1/3} - \frac{R_0}{\beta}, \tag{3}$$

where $\beta = 0.6$ is the entrainment coefficient and the source specific momentum flux is $F_m = \frac{\rho_0}{\rho_a}U_0^2\,r_0^2$. The equivalent source radius, $R_0 = r_0\sqrt{\frac{U_0}{U_a}\frac{\rho_0}{\rho_a}}$, is determined by matching the source mass flux of the plume to an equivalent flow of density ρ_a and velocity U_a [35]. The plume radius is given by $R = R_0 + \beta\,z$. Moreover, Briggs [16] argued that the rise enhancement due to the release of latent heat is rather modest. More precisely, the plume rises to a height only 10% to 20% greater than would be the case in the absence of latent effects. Plume behaviors under neutrally and stably stratified crosswinds are sketched in Fig. 11. In a stably stratified crosswind, the plume first reaches it maximum rise height then tends to a terminal rise height at a greater downwind distance. The approach to the terminal rise is not necessarily monotone; rather, some oscillation about the terminal rise height may occur—see also Fig. 17 below. The plume trajectory from the source to its maximum rise is described by

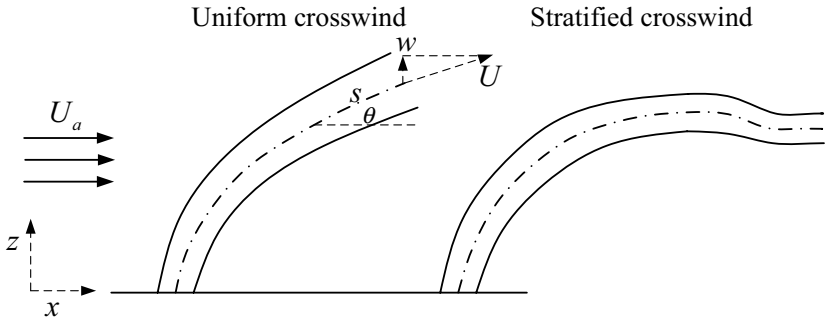

Fig. 11 Plumes under neutral (left) and stably stratified (right) crosswinds

$$z = \left[\frac{3\,F_b}{N^2\,\beta^2\,U_a} \left(1 - \cos\left(\frac{N\,x}{U_a} \right) \right) + \frac{3\,F_m}{N\,\beta^2\,U_a} \sin\left(\frac{N\,x}{U_a} \right) + \frac{R_0^3}{\beta^3} \right]^{1/3} - \frac{R_0}{\beta}. \tag{4}$$

The counterpart plume trajectory in an unstably stratified ambient where $N^2 < 0$ is expressed as

$$z = \left[\frac{3}{\beta^2\,U_a^2} \left(\frac{F_m\,U_a}{\sqrt{-N^2}} \sinh \frac{\sqrt{-N^2}}{U_a} x + \frac{F_b\,U_a}{-N^2} \left(\cosh \frac{\sqrt{-N^2}}{U_a} x - 1 \right) \right) + \frac{R_0^3}{\beta^3} \right]^{1/3} - \frac{R_0}{\beta}. \tag{5}$$

Davidson [37] argued that the above analytical solution yields predictions of the plume trajectory that are in good agreement with measurements, however, the dilution rate is overestimated and thus the visible plume length may be underestimated. By comparing the predictions of the analytical formulation with a set of sophisticated plume models e.g. Schatzmann ([126, 127]), Davidson revealed that the inclusion of an added mass factor or a drag term[6] in the momentum equation allows for accurate modeling of both the plume rise height and dilution rate. The added mass assumption derives from potential flow theory, which assumes that a plume accelerating through the ambient fluid can be regarded as having added mass attached its boundary. The amount of added mass is taken to be proportional to the core plume mass. Alton et al. [3] measured the trajectory and dilution rate of a hot water plume discharged into a crossflow in a water flume. They compared the experimental data with integral model predictions and verified Davidson's conclusion for simple analytical models.

[6] Briggs [16] preferred the added mass assumption over the inclusion of a drag term. The flow outside the plume is assumed to be irrotational thus the drag force term drops out in the momentum equation. Moreover, the assumption underlying the drag term is that there exists a turbulent wake on the leeward side of the "no-slip" surface of a solid object. By contrast, a plume consists of fluid so that its boundary with the ambient is more appropriately modeled as "free-slip". Briggs also listed some evidence that demonstrates the non-existence of the wake for bent-over plumes.

4.1.2 Advanced theoretical models

For improved predictions of plume behavior, integral models of greater complexity have been proposed. Instead of using a single entrainment term in the entrainment hypothesis, refined models incorporating two entrainment terms have been proposed by various researchers—see e.g. Hoult et al. [56] and Hoult and Weil [55]. The two-entrainment-coefficient assumption incorporates entrainment due to velocity differences both parallel and normal to the plume axis, i.e. $v_e = \gamma_1 \left| U - U_a \cos\theta \right| + \gamma_2 \left| U_a \sin\theta \right|$ where $U - U_a \cos\theta = w \sin\theta$ and γ_1 and γ_2 are the corresponding entrainment coefficients—see Tohidi and Kaye [141]. A modification to the above entrainment formulation was made by [2], i.e. $v_e = \gamma_1 \left| U - U_a \cos\theta \right| + \gamma_2 \left| U_a \sin\theta \right| \cos\theta$; the addition of $\cos\theta$ in the latter right-hand side term shuts off line thermal-type entrainment in the near source region. A more general entrainment relation proposed by Devenish et al. [40] reads

$$v_e = \sqrt[M]{\left(\gamma_1 \left| U - U_a \cos\theta \right|\right)^M + \left(\gamma_2 \left| U_a \sin\theta \right|\right)^M},$$

where $M \geq 1$. The entrainment assumption is further complicated by including the effect of ambient turbulence and a so-called drag hypothesis—see e.g. Winiarski and Frick [155], Wu and Koh [159] and Ooms and Mahieu [113].

Schatzmann [127] developed a model to predict the spreading and rising of buoyant jets in a stratified crosswind. A Gaussian profile was assumed for plume velocity, temperature and humidity. In contrast to the two-entrainment-coefficient models, four empirical constants were involved in the entrainment hypothesis. Schatzmann and Policastro [128] further advanced the aforementioned model by carefully quantifying the plume thermodynamics and the effects of stack downwash.[7] The pressure field around a bent-over plume in a crosswind is so complex that deriving a generic expression for the dynamic pressure gradient is extremely difficult. The error of assuming a zero dynamic pressure gradient is compensated by imposing a drag force normal to the plume axis [126]. To account for the downwash effects, additional terms are added to the drag force and the entrainment function to provide more bending and mixing due to the plume-wake interference. Schatzmann and Policastro [128] also include a shape factor in the drag coefficient (cf. their equation 18) to account for the non-circular plume cross section e.g. shown in Fig. 20 below. List [95] argued that Schatzmann's model is "probably the most appropriate technique for engineering design purposes". Schatzmann's model was further discussed by Davidson [36] using a parallel control volume formulation, and by Teixeira and Miranda [140] using a first-order turbulence closure in place of the entrainment assumption to improve the performance. Many integral models such as Hoult et al. [56] and Wu and Koh [159] produce unphysical results in some extreme cases, e.g. a momentum jet in a uniform co-flow (see the discussion in [126]), which Schatzmann's model avoids.

There are several other models that can be classified as advanced integral models. Carhart and Policastro [22] developed the Argonne National Laboratory and University of Illinois (ANL/UI) model to resolve some deficiencies of previous integral models e.g. the inability to correctly and simultaneously predict plume trajectory and dilution. Janicke and Janicke [64] proposed an integral plume rise model that is applicable for a

[7] Downwash describes the downward motion of effluent in the leeward wake zone. As a consequence of downwash, high-concentration, possibly harmful effluents can be transported to ground level [20].

three-dimensional wind profile and arbitrary source conditions. The added mass concept, rather than the drag hypothesis, was adapted in their formulation. Jirka [65] validated his four empirical entrainment coefficient model by comparison with experimental data for five distinct regime of buoyant jet flow i.e. pure jet, pure plume, pure wake, advected line puff and advected line thermal. More importantly, Jirka [65] pointed out the conditions beyond which integral models become invalid, e.g. the transition to a passive turbulent mixing plume, the final stage alluded to by [133]. Jirka [66] further extended his model to describe two dimensional buoyant jet flows.

Briggs [17] argued that most of the analytical models of plumes are based on conservation of mass, momentum and buoyancy and at least one closure assumption. Some models employ conservation of mean kinetic energy (cf. [118]), which is actually an alternative form of the momentum conservation equation. Various closure assumptions can be found in Table I of Briggs [16], which correspond to different conservation equations. In short, integral models provide a quick and efficient means of estimating the plume trajectory and dilution rate. However, a key restriction, as stated by Jirka [65], lies in the assumed unboundedness of the environment. For instance, and when the crosswind is sufficiently strong, cooling tower plumes may be drawn into the turbulent wake on the leeward side of the tower; such phenomena lie beyond the predictive capability of integral models.

4.1.3 Multiple sources and plume merger

For multiple sources in close proximity, several plumes may merge into a single plume with increased momentum and buoyancy. Following the "two-thirds" law, Briggs [17] argued that the maximum rise enhancement factor for n stacks was $n^{1/3}$, assuming all the buoyancies were combined completely. In fact, plume merger depends on many geometric and dynamic parameters that include the wind speed, wind direction and level of ground turbulence. To this end, Briggs's model for rise enhancement adapted results from available analytical models such as Murphy [111] and Anfossi et al. [7]. Wu and Koh [159] proposed a merging criterion for multiple plumes that emanate from adjacent cooling tower cells. They argued that the merged plume can be approximated by a central slot plume plus two half round plumes at the two ends. The effect of wind direction with respect to the tower arrangement was also included. Their predictions were in good agreement with the corresponding laboratory data on dry plumes. It should be emphasized that the merging criteria of Wu and Koh [159] is based entirely on geometrical considerations (Fig. 12a), and unfortunately, no physical justification is involved. Nonetheless, the conceptual simplicity offered by their model has led to its adoption in numerous studies of cooling tower plumes e.g. the ANL/UI model [22]. Modeling the induced flow into a turbulent plume using the complex potential of a line sink, Kaye and Linden [68] studied the coalescence of two pure axisymmetric plumes with equal and unequal source strengths (Fig. 12b). The point of coalescence is defined as the point where a single peak appears in the horizontal buoyancy profile. The distance between plume centers diminishes with height due to the passive advection of one line sink towards the other. The theoretically predicted merging height is somewhat larger than the value measured in analogue laboratory experiments; as Kaye and Linden [68] proposed, this mismatch is due to the sensitivity of the entrainment coefficient. Following the work of Kaye and Linden [68], Cenedese and Linden [23] proposed a piecewise model of plume merger accounting for various stages of plume interaction.

Lai and Lee [83] proposed a general semi-analytical model to account for the merging of an array of closely spaced buoyant jets. The induced flow was modeled using a distribution

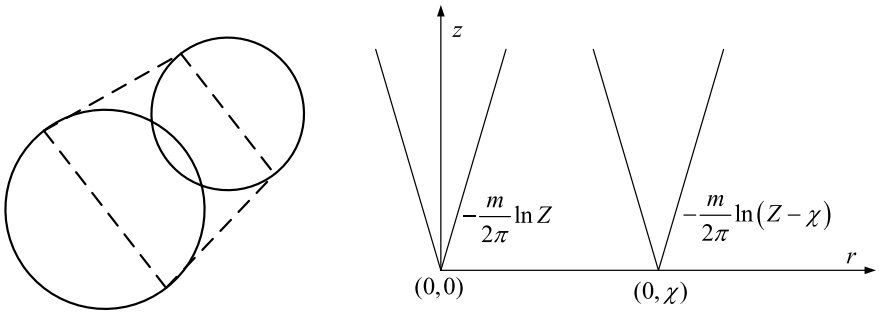

(a) Merging criteria by Wu and Koh [159]

(b) Approach of line sink by Kaye and Linden [68]

Fig. 12 **a** Plume merger occurs when the area of the central trapezoid bounded by dashed lines is the sum of the areas of the two half round plumes on both sides. **b** The induced flows into the two adjacent plumes are represented by link sinks $\Omega = -\frac{m}{2\pi} \ln Z$ and $\Omega = -\frac{m}{2\pi} \ln (Z - \chi)$, where $Z = x + \mathrm{i}y$ and m is the line sink strength

of point sinks. The velocity and concentration profiles in the merged jet (or plume) flow were obtained by momentum (or kinetic energy) and concentration superposition, and the corresponding results were validated by CFD simulation. Their predicted merging height for two pure plumes of unequal strength was compared with that anticipated by Kaye and Linden [68]—see Fig. 10b of Lai and Lee [83]. The method of Lai and Lee [83] yields better agreement with experimental data than does that of Kaye and Linden [68], especially when the buoyancy flux ratio between the two plumes is small. Moreover, their model can be extended to describe plume merger in a weak crosswind.

Rooney [120, 121] adapted the physical interpretation of velocity potential to approximate the plume-ambient boundary of single and multiple plumes. The model in Rooney [120], using a row of infinite line sinks, approached the limiting similarity solutions of axisymmetric and two-dimensional plumes or jets below and above the merging height. Further in Rooney [121], he studied the merging of plumes with sources placed along the perimeter of a circle; the theoretical predictions agree satisfactorily with the experimental results of Cenedese and Linden [23]. One restriction of Rooney's models is that the plume source is assumed to be small compared to the separation distance between neighboring plume centers. However, industrial cooling towers typically have large diameters (~10 m) and they are usually closely spaced. Recently Li and Flynn [90] modified Rooney's theory to consider the merger of non-ideal plumes with arbitrary source diameter. Li and Flynn's theoretical predictions of merging height agree well with the earlier predictions of Wu and Koh [159]. In case of a crosswind, the bent-over plume can be simulated as a line doublet [158] so that Rooney's theory may be extended to a windy environment.

4.2 CFD models (single and multiple sources)

CFD simulation can describe almost all aspects of cooling tower plumes, including recirculation, downwash, plume merger and condensation/evaporation. Like their integral model counterparts, CFD models require closure, i.e. in the form of a turbulence model. A quick comparison between the different kinds of turbulence models that have been applied to

atmospheric plumes is summarized in Table 4.4 of Andersson et al. [4]. The CFD models reviewed here are mainly Reynolds-averaged Navier–stokes (RANS) models.

Demuren and Rodi [39] used a 3D computational model to resolve the complex flow field past a cylindrical cooling tower whereby the downwash effects under strong crosswinds was modeled. Their pioneering work used a k-ϵ turbulence model [87] and reproduced flow patterns in the vicinity of the tower. They modeled plume downwash and the formation and decay of longitudinal vortices—see their Fig. 20. One shortcoming of their model is the underestimation of the buoyancy effect on plume rise in the near field.

Becker et al. [12] proposed a unique numerical model of cooling tower plume recirculation. The flow inside the tower was treated as a porous media flow whereby each of the cooling tower components, e.g. fill racks and drift eliminators, was modeled as a different porous medium of a different hydraulic mass conductivity. Meanwhile, the wake zone downstream of the tower was resolved using the Navier–Stokes equations. The flow fields inside and outside the cooling tower were coupled by matching the pressures and mass flow rates at the louvers. The amount of recirculation[8] was defined as

$$\text{Recirculation} = \frac{\bar{t}_{\text{in}} - t_a}{\bar{t}_{\text{out}} - t_a}, \tag{6}$$

where t denotes temperature, the overbar denotes mass average and the subscripts 'in' and 'out', denote, respectively, the flows entering the louvers and leaving the cooling tower (the subscript 'a' indicates the ambient). As the wind speed increases, the plume is quickly bent towards the leeward side of the tower and is subsequently entrained into the wake zone thus enhancing recirculation. There results a decrease in the effluent temperature before it is discharged into the wake zone, which has the effect of then diminishing the recirculation. The findings of Becker et al. [12] confirmed these two opposing effects and predicted an increasing then decreasing trend of recirculation with increasing wind speed. Later Ge et al. [46] studied the effects of recirculation on the visible plume potential using CFD modeling. Their results showed that recirculation can increase the fogging frequency, which subsequently increases the heating demand for plume abatement. The heating demand for a recirculation ratio (defined by 6) of 20% is 80–90% greater than that without recirculation.

Bornoff and Mokhtarzadeh-Dehghan [14] investigated the interaction of two adjacent plumes in tandem and side-by-side arrangements in a crosswind. The turbulence model was a low Reynolds number k-ϵ model; the eddy viscosity was damped in the energy dissipation (ϵ) equation when the local Reynolds number was low. Their simulations indicated that the tandem configuration leads to rapid merging and a corresponding rise enhancement. Conversely, when the plumes are located side-by-side, their interaction is dominated by counter-rotating vortex pairs. The numerical results of Bornoff and Mokhtarzadeh-Dehghan [14] are consistent with the later experimental study of Contini et al. [31], which identified the effects of counter-rotating vortex pairs on the mixing and rise of adjacent plumes. König and Mokhtarzadeh-Dehghan [78] used the standard k-ϵ turbulence model and a finite volume method to simulate multiple plumes emitted by a four-flue chimney. By comparing the results of multiple plumes with those of a single plume of the same overall source volume flow rate, they revealed that significant differences of velocity, temperature and turbulent energy occur only in the early stages of plume rise and spread. Notably, the multiple plumes merge into a single plume within ten stack diameters of the chimney.

[8] A summary of different definitions to recirculation can be found in Liu and Bao [96].

Mokhtarzadeh-Dehghan et al. [105] modeled two interacting field-scale dry plumes in a neutral crosswind using three different turbulence models, i.e. the standard k-ϵ model, the renormalization group (RNG) k-ϵ model [160] and the Differential Flux Model (DFM). The constants in the turbulence models and the discretization schemes are summarized in their Tables 1 and 2, respectively. The numerical results of Mokhtarzadeh-Dehghan et al. [105] showed general agreement in the plume rise height for all three models, of which DFM obtained temperature profiles in better agreement with experimental results.

Takata et al. [136] used an RNG k-ϵ model to study the visible plume behavior above a mechanical draft wet cooling tower. The turbulent Prandtl number and Schmidt number were both set to 0.9. Moreover, the measured average velocities in three directions and the turbulent energy at the fan exit were used as the boundary conditions for the simulation. Results showed that the predicted length, width and volume of the visible plume agree with the corresponding measured values within 20%. Later Takata et al. [137] adapted the same CFD model to predict the visible plume region above a hybrid crossflow wet/dry cooling tower. The initial and boundary conditions are exhibited schematically in Fig. 13. Their results showed that the fan can completely mix the wet and dry air streams, and the predicted dimensions of the visible plume agree with observations with an error range of 15% to 20%. Furthermore, their CFD analysis revealed that the effect of the ambient wind on the dimension of the visible plume is significant—see Fig. 14.

Brown and Fletcher [18] investigated the effect of condensation on plume rise. A buoyancy-corrected k-ϵ turbulence model was adapted. Meanwhile, a separate algorithm was developed to model the evaporation/condensation process. Consistent with Briggs [16], their results showed that condensation does not affect significantly plume rise and ground level odour.

A full 3D CFD model on natural draft wet cooling towers is detailed in Klimanek [72]. The dispersed RNG k-ϵ model, which is a type of multiphase k-ϵ model, was selected for turbulence closure. Whereas Takata et al. [137] did not specifically simulate cooling tower processes, Klimanek studied such processes in detail. For instance, heat and mass transfer processes within the fill zone were modeled using proper orthogonal decomposition coupled with radial basis function networks, which is characterized as a simplified and reduced order model [74]. The slight contraction of the plume near the stack exit seems to indicate that the plume is initially lazy with an excess volume flow rate versus a pure plume [60]. Later Klimanek et al. [75] used the 3D model of Klimanek [72] to simulate a natural draft wet cooling tower with flue gas injection which included the effect of crosswind on rising plumes. Figure 15 shows that a recirculation zone forms at the windward side of the tower outlet, which leads to a possible reduction in the air flowrate through the tower.

Chahine et al. [24] also modeled the effect of wind on cooling performance and plume behavior above natural draft wet cooling towers, however, using a different numerical approach compared to Klimanek et al. [75]. The heat, mass and momentum transfer processes within the fill zone were parameterized using a source term approach. Specifically, the heat gain of air, mass loss of water and momentum loss of air through the fill zone were expressed as source terms in the conservation equations of thermal energy, mass and momentum, respectively. Moreover, the liquid potential temperature was used in the thermal energy conservation equation at the scale of the atmospheric boundary layer. Their predicted vertical profiles of plume temperature, velocity and liquid water content agreed well with field measurements.

Hargreaves et al. [51] proposed a simplified CFD analysis of plumes in a quiescent atmosphere using a k-ϵ model. The accuracy of their model was demonstrated by

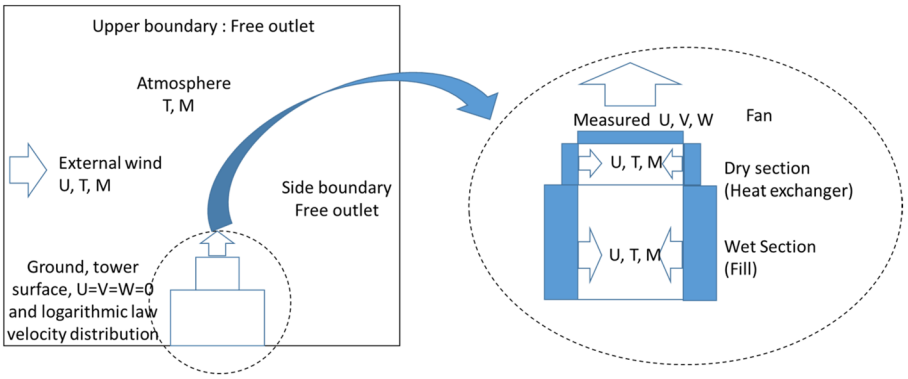

Fig. 13 [Gray scale] Initial and boundary conditions used in the CFD simulation of Takata et al. [137]. The fan exit velocity distributions (U, V and W) measured in Takata et al. [136] are used as the velocity boundary conditions. Measured ambient dry- and wet-bulb temperatures and the wind speed are also used as the boundary conditions. The exiting air velocity, temperature and moisture of the wet and dry sections are determined from design calculations. (Figure taken from [137])

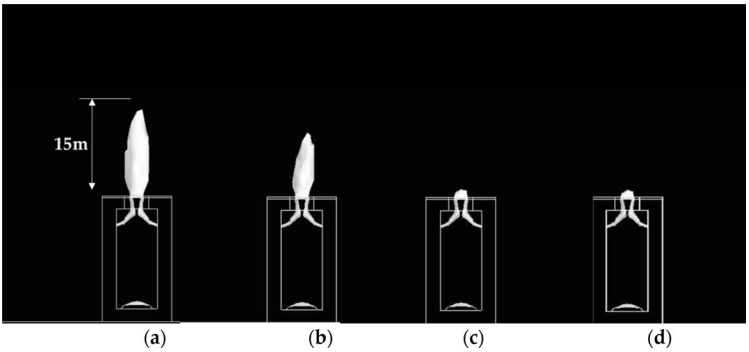

Fig. 14 [Gray scale] Effect of wind speed on the scale of the visible plume produced above a hybrid wet/dry cooling tower; wind speeds of (a) 0, (b) 1m/s, (c) 3 m/s and (d) 5 m/s are considered. (Figure taken from [137])

comparison with the theory of MTT and the empirical profiles of vertical velocity and reduced gravity by Rouse et al. [122]. Notably, their model predictions showed that MTT applies only at a distance well above the source—see their Fig. 17 for a comparison of plume centerline velocity predicted by the respective CFD and MTT models. The model of Hargreaves et al. [51] is much less computationally expensive compared to large-eddy simulation (LES) while maintaining a reasonably good description of the flow.

4.3 Similitude laboratory experiments (single and multiple sources)

To corroborate the predictions of analytical and numerical models, a number of similitude experiments of cooling tower plumes have been completed. Laboratory experiments enjoy a number of advantages. For example, wind tunnel experiments can easily simulate the

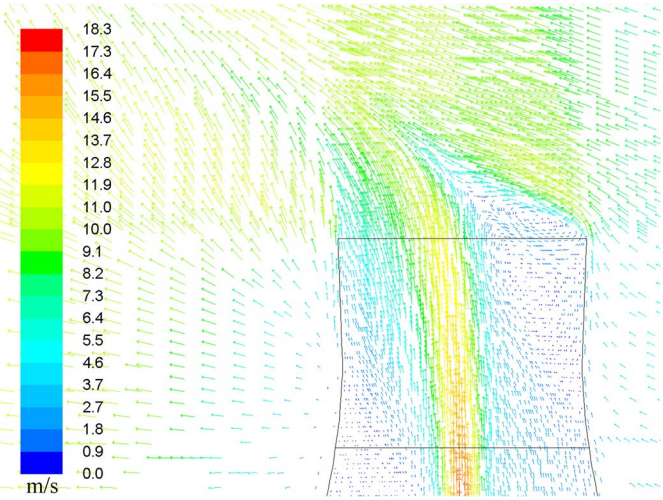

Fig. 15 Plume velocity vector map near the tower exit in a crosswind. (Figure taken from [75])

impact of neighboring and complex terrain. Andreopoulos ([5, 6]) conducted wind tunnel experiments on cooling tower plumes considering both uniform and non-uniform crossflows. In the former case, strong interactions between the bending plume and the wake zone of the cooling tower were found, which served as the main reason for stack downwash. Downwash was observed to be relatively strong at low velocity ratio (stack exit velocity to crossflow velocity) and high Reynolds numbers (defined based on the crossflow velocity and stack exit diameter). Michioka et al. [104] proposed a novel method of using wind tunnel experiments to predict the visible plume region above a wet cooling tower. A tracer gas was used to model the effluent emitted from the cooling tower and the subsequent dispersion of water vapor in the atmosphere. The validity of this method was confirmed by the fact that the predicted visible plume length and height are in good agreement with field observations [103]. On the basis of Michioka et al's approach, Guo et al. [49] performed wind tunnel experiments to study plume rise and the visible plume region of a natural draft cooling tower. Their predictions of plume rise agree with Briggs' two-thirds law for downstream distances of 50 m to 200 m. Furthermore, their measurements of the visible plume region are consistent with the simulation results of Policastro and Wastag [115].

Contini et al. [33] used wind tunnel measurements to analyze the variance, skewness, kurtosis, intermittency, probability density function and power spectrum of the concentration field in two merging plumes. Consistent, broadly speaking, with Slawson and Csanady [133] , their results identified three distinct phases of plume development. In sequence, the three phases are dominated by turbulence self-generated within the plume near the stack, by both internal and external turbulence at somewhat greater distances and by external turbulence at further downwind distances.

Liu and Bao [96] extended the above studies by considering, in the wind tunnel context, not only plume rise and ambient turbulence but also recirculation. Their set-up is illustrated in Fig. 16. Flow visualization was made possible by putting dry ice within the cooling towers; the water vapor in the air flow was quickly cooled to the dew point causing condensation. Separately, carbon monoxide (CO) was released into the central region of the cooling tower; from measurements of the CO concentration at the tower inlet and outlet, estimates

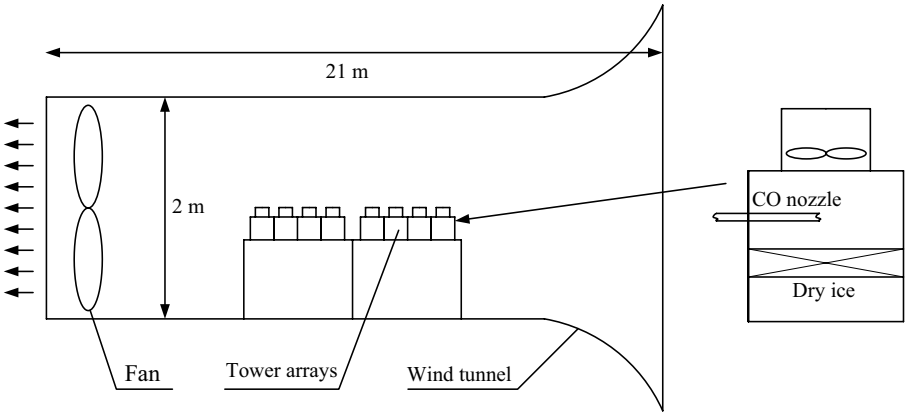

Fig. 16 Wind tunnel experimental set-up of Liu and Bao [96]. Dry ice is put inside each cooling tower cell for flow visualization. Carbon monoxide is used as a tracer whose concentrations at the inlet and outlet of the tower are measured to determine the recirculation ratio

of the recirculation ratio were made. As a result of their experimental findings, Liu and Bao [96] proposed an empirical formula that expresses the recirculation ratio as a function of the following parameters: the length of the cooling tower row, the angle between the tower array and wind direction, the distance between two neighboring tower arrays, the height of the air intake and the wind speed. To minimize the recirculation ratio, several recommendations are made, such as to align the long axis of the tower array parallel to the dominant summertime wind direction (a practice common in industry), to shorten the length of tower array and to maintain a distance between tower arrays that is four to five times the air intake height.

Another powerful experimental tool is the water tank experiment. Here, flow visualization can be achieved using colored dyes and an ambient stratification may be realized using salinity gradients. Using a water tank, Davis et al. [38] investigated the dilution characteristics of single and multiple buoyant discharges in a stationary ambient. Their simultaneous measurements of velocity and salinity within the plumes indicate that entrainment is greatly increased by reducing the source densimetric Froude number (defined as $\mathrm{Fr} = U_0/\sqrt{g\frac{\Delta\rho}{\rho_a}D_0}$ where U_0 is the nozzle exit discharge velocity, g is gravitational acceleration, $\Delta\rho$ is the density difference between the jet centerline and ambient whose density is ρ_a and D_0 is the nozzle diameter). Contini and Robins [29] studied the rise and evolution of a single buoyant plume and a pair of in-line plumes in neutral crossflows using a towing tank apparatus. Flow visualization and local concentration measurements were used to investigate the plume trajectory and plume interactions particularly for two in-line plumes. A later study also by Contini and Robins [30] considered two adjacent buoyant plumes while imposing various wind directions. More recently, Contini et al. [32] provided a detailed comparison between several plume rise models and water tank experimental data for neutral and linearly stratified crossflows. The measured plume trajectory (see e.g. Fig. 17) was used to find, using statistical means, the appropriate entrainment coefficients in various plume models—see their Tables 3 and 4. Furthermore, Contini et al. [32] found that the added mass concept generates improved predictions of the maximum rise height and subsequent oscillation frequency. Another finding was that the measured plume oscillation was more significantly damped than was predicted theoretically. This may, in

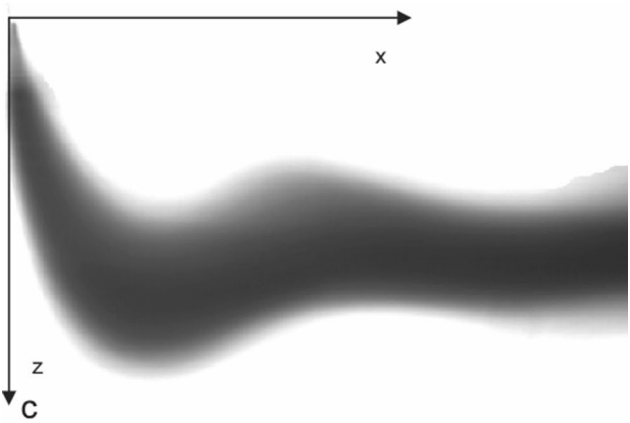

Fig. 17 A water channel experimental image of a plume in a stably stratified cross-flow [32]. The plume starts to oscillate after reaching its maximum rise height. (Figure taken from [32])

fact, speak to the influence of radiating internal gravity waves—see e.g. the LES study of Devenish et al. [40].

Instead of using the tow tank technique that mimics the effect of a laminar crossflow, Macdonald et al. [98] conducted water flume experiments to study the rise behavior of a pair of merging plumes. The advantage of a water flume compared to a tow tank set-up is that the atmospheric boundary layer flow can be simulated properly only in the former case. The key result revealed by Macdonald et al. [98] is that the best tower arrangement is in-line with the wind direction for the maximum rise enhancement; the worst tower arrangement is perpendicular to the wind direction wherein there is little or no rise enhancement compared to the single source case. As discussed in Hensley [53], the perpendicular configuration is also more likely to induce motions like recirculation and/or downwash.

4.4 Plume in a turbulent environment

Ambient turbulence (if present) becomes dominant over the plume's self-generated turbulence only at some further downstream distance from the source. Briggs [17] proposed two patterns of turbulence, i.e. mechanical and convective turbulence as illustrated schematically in Fig. 18. Figure 18a illustrates mechanical turbulence created by wind flowing around roughness elements, whose size is one of two key factors in setting the turbulence intensity; the flow speed is the other. Figure 18b illustrates convective turbulence due to ground heating. The intensity of convective turbulence depends on the sensible heat transfer rate from the ground to the air and the depth over which an overturning of the air takes place. Briggs [17] argued that the large scale turbulent eddies can push plume segments down to the ground and the small scale eddies can enhance mixing between the plume and the ambient. Simple analytical models of plume rise affected by mechanical and convective turbulence were proposed and discussed in section 8-5 of Briggs [17]. Three different forms of entrainment velocity due to ambient turbulence are summarized in Table 2 of Briggs [16], of which the one preferred by Briggs is given by

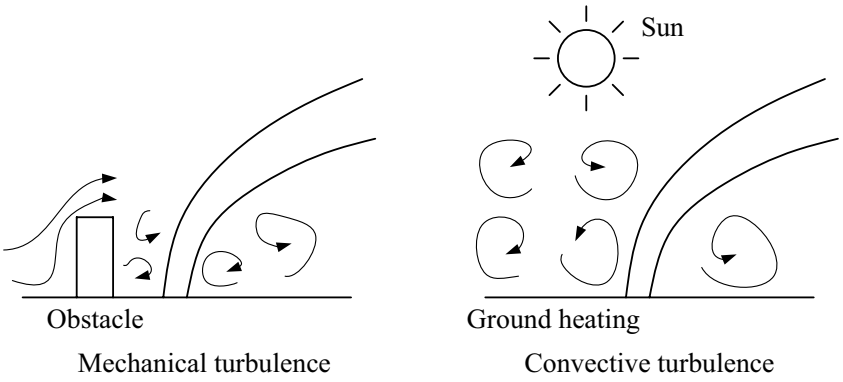

Fig. 18 Schematics of mechanical and convective turbulence

$$v_e \propto \left(\epsilon_a R\right)^{1/3}, \tag{7}$$

where ϵ_a is the turbulent energy dissipation rate and R is the plume radius. Equation 7 is based on the assumption that the effective eddies are in the inertial sub-range of the turbulence spectrum where the turbulence statistics depends only on ϵ_a. Also implied by 7 is the fact that $R \ll l$ where l is the dominant eddy size associated with ambient turbulence.

Turner [143] formulated a theoretical model to account for both the inflow of ambient air by turbulent entrainment into the plume and the outflow of plume fluid due to turbulence in the environment. Specifically, his theory followed MTT but introduced a constant mean outflow (extrainment) velocity. Theoretical results showed that the plume width first increases then decreases and finally disappears within a certain downstream distance. The physics of the decreasing profile is questionable, thus the model of Priestley [117] was adapted by Turner [143] after the plume reaches its maximum width. (At this maximum width, the turbulence within the plume or thermal is regarded as a part of the environmental turbulence). The laboratory experiments of Turner [143] simulating a neutral environment revealed that the outflow velocity is of the same order of magnitude but somewhat less than the r.m.s. turbulent velocity. As stated later by Netterville [112], Turner's novel contribution was the stringent definition of the "active" radius of the plume or thermal to include only that portion governed by the buoyancy force and exhibiting a systematic upward motion.

Hamza and Golay [50] constructed a model of moist plumes in the atmosphere whereby atmospheric turbulence is accounted for by incorporating a one-dimensional planetary boundary layer (PBL) model. As sketched in Fig. 19, the plume was modeled using the integral model of Winiarski and Frick [155] and a numerical (k-ϵ turbulence) model, with the dividing line (vertical dashed line in Fig. 19) representing the point of model crossover. Given vertical profiles of temperature, humidity and wind speed, the one-dimensional PBL model yielded the vertical Reynolds stress and turbulent heat flux distribution, which served as inputs into the numerical plume model. The test results demonstrated their model strength in complex atmospheric conditions under which integral models may have difficulty.

Netterville [112] proposed a two-way entrainment model for plumes in turbulent winds, which combines the methods of Priestley [117] and Turner [143]. A characteristic frequency is introduced to quantify the decay rate of the vertical momentum and buoyancy,

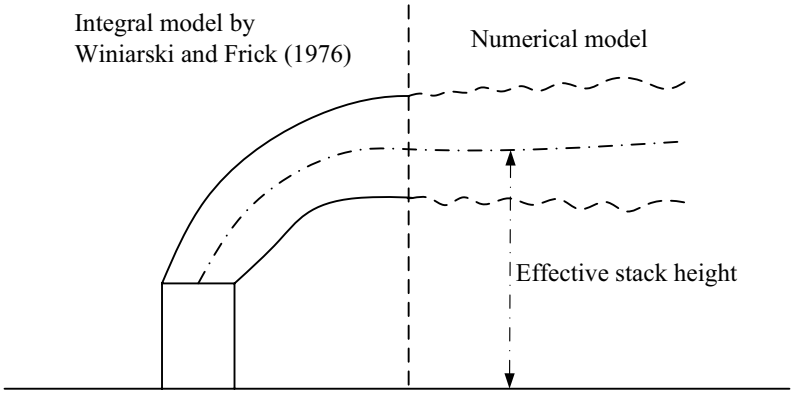

Fig. 19 Division of plume modeling suggested by Hamza and Golay [50]. The effective stack height, $h_{\text{eff}} = h_{\text{stack}} + l_{\text{b}}$, where h_{stack} is the stack height measured from the ground and l_{b} is a so-called buoyancy length defined as the radius of curvature of a pure plume at the stack exit

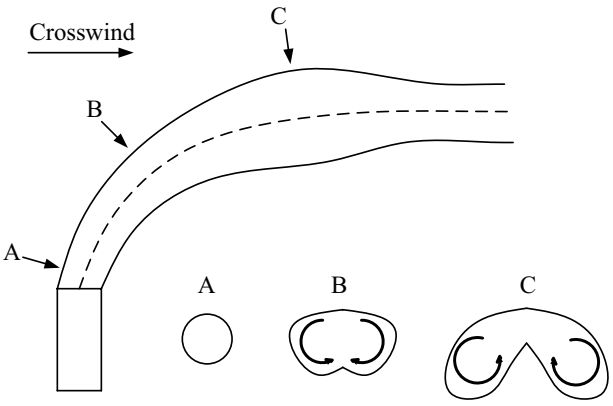

Fig. 20 Vortex motion at different elevations of a plume in a crosswind. At cross section A, the plume behaves like a jet that has a circular cross section. At this stage, the plume's self-generated turbulence is dominant in the dilution process. At cross section B, the edge of the plume is sheared off by the wind thus resulting in a kidney-shaped cross section. Thereafter at cross section C where the plume is fully bent-over, the dilution process is dominated by the interaction between the two counter-rotating line vortices and the ambient crossflow [43]

which justifies the governing equations introduced by Djurfors [41]. The new model outperforms the "laminar" plume model at downwind distances beyond 1 km where the effect of atmospheric turbulence (assumed homogeneous and isotropic by [112]) is dominant. Later Gangoiti et al. [45] adapted Netterville's parameterization of entrainment but argued that a wind-sheared atmosphere makes more sense than a flat wind profile, because atmospheric turbulence must be fed by wind shear to maintain its stationarity.

Huq and Stewart [62] compared the plume evolution in laminar and weakly turbulent crossflows by laboratory experiments. The turbulent environment was produced by locating a turbulence generating grid upstream of the plume source. They found that the decaying, grid-generated turbulence enhanced the dilution of the buoyant plume core by up to

33%, even though the associated dissipation rates were approximately two orders of magnitude smaller than the plume turbulence dissipation rates. Not surprisingly, the turbulent crossflow was also found to decrease the plume rise height, which can be accounted for by adopting a modified entrainment coefficient, i.e. β in 3.

HÜbner [59] conducted comprehensive experiments of a buoyant plume in a turbulent environment, where the ambient turbulence was created using an oscillating grid. Such a turbulent environment is nearly isotropic, horizontally homogeneous and exhibits intensity that increases closer to the grid. Two processes, plume meandering[9] and plume spreading (see his figures 5.9b and c), are modeled distinctly. Lai et al. [84] studied experimentally the dynamics of buoyant jets in an ambient characterized by homogeneous and isotropic turbulence. The observations summarized in Lai et al.'s study are consistent with those of HÜbner [59]: the large-scale eddies in the ambient turbulence tend to cause plume/jet meandering, whereas the smaller eddies with size comparable to the plume/jet characteristic length scale tend to affect the internal structure of the plume/jet. For buoyant jets, Lai et al. [84] found that the mixing characteristics are governed by a critical length scale and the densimetric Froude number. This former length scale, in the case of a pure plume, is expressed as

$$l_{\mathrm{cp}} = \left(F_0/\epsilon_a\right)^{1/2}, \tag{8}$$

where F_0 is the source buoyancy flux. l_{cp} is interpreted physically as the height where the velocity of the ambient eddies with size comparable to the plume diameter is close to the mean entrainment velocity of the plume; beyond l_{cp}, the plume mixing is expected to be influenced by the ambient eddies. In terms of integral modeling, Lai et al. [84] argued that the second-order turbulence statistics, which are unimportant in the case of a plume rising through a quiescent ambient (see e.g. the MTT model), become important insofar as the ambient turbulence exerts an order-one influence on the plume mixing. Therefore, the associated second-order terms must be included in the plume equations.

Witham and Phillips [157] studied the dynamics of turbulent plumes under convective turbulence. Their theoretical model adapted the theoretical approach of Turner [143] and complemented the theory of Netterville [112]. Meanwhile in their experiments, a negatively buoyant saline plume was initially seeded with hydrochloric acid of pH 1.2 versus an ambient pH of 7.1. For relatively small ambient velocities, their measurements showed that the pH of the plume boundary drops rapidly below 6.3 approximately four nozzle diameters downstream, which demonstrates that plume fluid is extrained into the turbulent surroundings. A quantitative comparison between the theoretical plume length (defined as the vertical distance where the plume radius diminishes to zero) versus its experimental counterpart showed good agreement. The comparison also yields the best-fit entrainment and extrainment coefficients. Extended study of plumes in finite convecting environments reveals the importance of convective mixing at the density interface that forms in filling-box type flows, e.g. of the type considered by Baines and Turner [10], Baines [11] and Kaye et al. [69].

[9] Meandering describes the process by which the buoyant plume centerline deviates from the perfect vertical when discharged into a turbulent environment.

4.5 Plume bifurcation

As shown in Fig. 20, Scorer [130, 131] argued that bifurcation results from counter-rotating vortex pairs of equal strength but opposite sign within a bent-over plume. Some qualitative results by Scorer are: (1) bifurcation is always clearly present in cases of hot plumes rising in smooth winds, and, (2) bifurcation can be induced by cooling at the plume boundary. The latter case occurs when the plume is visible, and the mixing between the ambient (unsaturated) air with the supersaturated air at the plume boundary evaporates and disperses the liquid moisture. Thus the cold flow at the plume edge falls due to its negative buoyancy. The associated baroclinic torque can enhance both the peripheral circulation exhibited schematically in Fig. 20 (points B and C) and also the tendency to plume bifurcation. In discussing Scorer's conclusions, Briggs [15] stated "it is not clear under what conditions the two vortices can separate, however, bifurcation is rare and appears to occur only in light winds".

In analogue laboratory experiments conducted in a water channel, Hayashi [52] found that the plume tends to bifurcate as it approaches the free water surface, which corresponds to the bottom of a temperature inversion in the context of atmospheric convection. A subsequent reanalysis of Hayashi's experimental data by Khandekar and Murty [70] determined that the free water surface creates an "image effect" [82], which leads to the lateral separation of the vortex pair (see Fig. 21). Khandekar and Murty [70] proposed that the image effect depends on the location and strength of the inversion layer and the buoyancy flux of the plume. Overall, and in agreement with the assertion of Briggs [15], bifurcation caused by a separation of vortices may be considered as a rare phenomenon. Abdelwahed and Chu [1] extended Hayashi's experiments and found that a bifurcated jet follows the same generic scaling law as its non-bifurcated counterpart. Jirka and Fong [67] proposed a theoretical model that superimposes the internal vortex dynamics upon an integral model of buoyant jets in crossflows, the integral model being similar to that described in the follow-up study by Jirka [65]. The interaction of the counter-rotating motion with a fluid boundary and/or density interface was modeled by Jirka and Fong [67] as a repulsive force that leads to bifurcation.

Turner [142] treated the flow within a bent-over plume in a uniform ambient as a vortex pair. He assumed that the circulation, Γ, around one line vortex, is constant, thus the momentum (or impulse) of the vortex pair is proportional to the separation distance of the pair. In this way, any increase of momentum due to buoyancy leads to separation of the vortices. Furthermore, his theoretical result showed that the separation distance is linearly related to the downwind distance, which agrees well with experimental observations. It is, however, expected that Turner's theory may not apply for stratified environments.

Bennett et al. [13] used a scanning-Lidar system to measure the plume rise height, temperature profile, wind speed and direction, and the measured plume rise height is compared with Briggs' formula. They found that plume bifurcation is favored in case of low ambient turbulence in a stable boundary layer. Moreover, and in contrast to Abdelwahed and Chu [1], their measurements showed that bifurcation leads to a reduction in plume rise height due to the reduced buoyancy flux after plume splitting.

Ernst et al. [42] analyzed bifurcation using ideal flow theory and thereby concluded that it is an induced lateral lift force that causes the vortices to separate. Their complementary laboratory experiments showed that bifurcation occurs for bent-over and straight-edged (i.e. slightly bent-over) buoyant jets for initial jet-to-crossflow velocity ratios of between

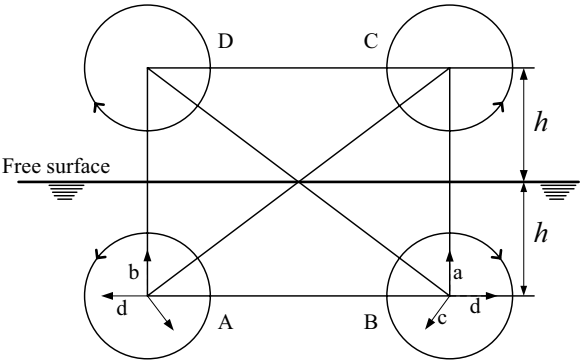

Fig. 21 Image effect of the free surface on the vortex pairs A–B. The free surface acts as an image plane in which the vortex pairs A–B are mirrored, thus creating the image vortex pairs C–D. The velocity induced at vortex A (or B) by the other vortices B, C and D (or A, C and D) is vectorially represented using the corresponding lower-case letters. Note that the resultant horizontal velocity vectors at vortex A are opposite to those of vortex B, which leads to the separation of the vortex pairs [42]

two and six. For even larger jet-to-crossflow velocity ratios, bifurcation is blurred by the spreading gravity current that forms as the buoyant jet approaches the free water surface.

Huq and Dhanak [61] studied experimentally the conditions under which the bifurcation of a circular jet in crossflow arises. They concluded that bifurcation occurs at some finite distance from the source if the initial mean jet-to-crossflow velocity ratio is greater or equal to four. In turn, the distance from the source where bifurcation initiates increases with the jet-to-crossflow velocity ratio.

Arakeri et al. [8] investigated the occurrence of bifurcation in case of horizontal injection of a laminar water jet into a brine solution. They found that bifurcation occurs in jets of relatively high Schmidt number and is caused by the slow moving fluid at the edges of the jets.

Cintolesi et al. [26] performed LES simulations of buoyant jets in a neutral crossflow. Their simulations reproduced the counter-rotating vortex pair in the entrainment region where crossflow dominates over the initial momentum and buoyancy. Notably, a sausage-like turbulent structure develops at the top boundary of the plume. Moreover, these structures appear only in buoyant plumes but not in non-buoyant jets, which indicates that buoyancy tends to supply energy for the rotational motion within the plume.

In general, it seems that the mechanism of bifurcation is incompletely understood. Although the pressure distribution of the vortices proposed by Ernst et al. [42] gives a reasonable hypothesis, rigorously speaking, a plume cannot be regarded as a rigid body. Scorer [131] argued that bifurcation is due to a buoyancy induced circulation, however, buoyancy must obviously be omitted in the context of jet bifurcation [1, 61]. Lavelle [88] argued that the large number of potential factors, such as background stratification, rotation and boundary layer shear, make difficult the task of determining exactly when plume bifurcation will arise. In terms of atmospheric dispersion, plume bifurcation enhances the dilution rate, albeit at the cost of possibly reducing the plume rise height.

4.6 Cooling tower drift

Cooling tower drift consists of water droplets mechanically entrained into the air flow through a wet cooling tower and discharged along with the moisture-laden buoyant plume. The US EPA considers cooling tower drift as a particulate emission [94]. In this vein, it is important to highlight that only $\sim 1\%$ of the drift exhausted by a cooling tower is of respirable size i.e. has a diameter less than 5 µm [19].

Roffman and Van Vleck [119] and Chen [25] reviewed the measurement techniques and theoretical models concerning drift deposition. In general, drift deposition is influenced by several physical processes, i.e. the dynamics and thermodynamics (evaporation) of droplets, droplets falling from a rising plume and dispersal by atmospheric turbulence. Chen [25] compared 10 published theoretical models of drift deposition and found that the predicted maximum deposition and the corresponding downwind location deviate by two and one order of magnitude, respectively. These discrepancies, as argued by Chen [25], are due to the different assumptions concerning the plume's vertical velocity as a function of height, and the effective height of emission i.e. the maximum rise height of droplets. A complete database for model validation can be found in Laulainen et al. [86], which encompasses the simultaneous measurements of cooling tower source characteristics, e.g. drift rate, drift droplet size distribution, and meteorological conditions. Different drift measurement methods such as droplet impaction and the application of cyclone separators were compared in Golay et al. [47]. Golay et al's study revealed that there are nontrivial differences in the drift measurements when different methods are applied.

More recent studies on drift have focused on drift deposition and making use of CFD tools. For example, Meroney [101] developed a CFD code to predict cooling tower drift deposition downwind of a cooling tower. The advantage of Meroney's CFD model as compared to previous analytical methods is that it accounts for the effect of downwash. The turbulence model was the standard k-ϵ model, but [101] also argued that the RNG or realizable k-ϵ models [132] might be preferred in cases of shorter mechanical draft cooling towers and/or surrounding structures. The source droplet size distribution was modeled using a Rosin-Rammler particle distribution through the fitting of published data—see Table 1 of Meroney [101]. The trajectories of drift droplets as a discrete phase were resolved using a Lagrangian stochastic approach. Later Meroney [102] tested the CFD model of Meroney [101] for urban cooling towers with surrounding buildings. One deficiency of Meroney's CFD model is that the effect of droplet evaporation was not accounted for. This particular deficiency was corrected in the follow-up CFD model developed by Lucas et al. [97]. They investigated the influence of ambient conditions on the drift deposition of a natural draft cooling tower. A k-ϵ turbulence closure was employed to model the plume flow as a continuous phase, whereas a Lagrangian formulation derived from momentum and energy conservation was employed to describe the drift droplets as a discrete phase. Model performance was validated by comparison with other analytical, CFD and observational results as illustrated in Fig. 22. A key result from their study is that the drift deposition rate decreases with decreasing ambient humidity ratio, increasing droplet exit temperature and, most especially, increasing ambient dry-bulb temperature. Later Consuegro et al. [28] adapted a similar CFD model but considered mechanical draft cooling towers in urban areas. Their study revealed that buildings downstream of the tower impose negligible influence on the area affected by drift deposition.

Sánchez et al. [125] studied the lifetime of drift with the combined effects of atmospheric conditions and droplet size distribution. If the lifetime experienced by the droplets is

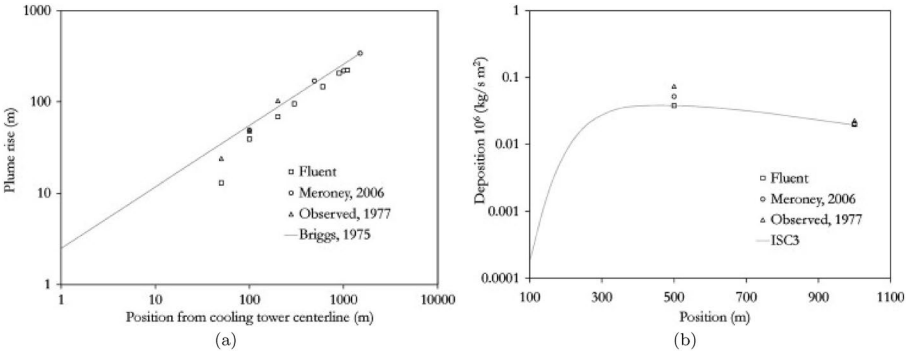

Fig. 22 **a** Plume trajectories from Lucas et al. [97], Meroney [101], the 1977 Chalk Point Dye Tracer Experiment and Briggs' plume rise formulae. **b** Drift deposition rates (mass/area/time) from Lucas et al. [97], Meroney [101], the 1977 Chalk Point Dye Tracer Experiment and the Industrial Source Complex (ISC3) Dispersion Models. The definition of drift deposition rate in CFD simulations is given in Meroney [101]. (Figure taken from [97])

less than the time necessary to reach ground level, there is obviously less risk of Legionella bacteria. Their CFD model is similar to the modeling of continuous and discrete phases by Lucas et al. [97]. On the other hand, they measured the meteorological conditions and droplet size distribution and temperature from a pilot mechanical draft cooling tower as the boundary conditions for their numerical model. Meanwhile, the measured deposition was used for validating their numerical model. Results from the study of Sánchez et al. [125] were broadly consistent with those of Lucas et al. [97]; they revealed that a short lifetime is favored under conditions with high ambient temperature, low relative humidity and small droplet size.

5 Conclusions

The present manuscript gives a summary of plume abatement approaches and the modeling of buoyant moist plumes. Both traditional and novel plume abatement approaches are reviewed. Sensibly heating the hot, humid air so as to reduce the exhaust relative humidity has been studied by several researchers on cooling towers used in HVAC systems. Solar collectors and heat pumps are considered as potential heat sources, however, the intermittency of solar energy (and its complete absence at nighttime) poses obviously challenges. A conventional PPWD tower adds a dry section through which the ambient air is sensibly heated and thereafter mixed with the hot, humid air from the wet section, thus the resulting air mixture is discharged with lowered relative humidity. For PPWD counterflow towers, static mixers are usually inserted within the plenum chamber to promote the mixing of the wet and dry airstreams. These static mixers range from simple baffles to vortex generators. The latter can achieve good mixing efficiency with moderate pressure drop. On the other hand, flow deflectors, though they increase the pressure drop and hence fan power, are generally more suitable for back-to-back cooling towers. A further option is to enhance mixing using a stirring device. Another approach, originally found in PPWD crossflow towers, is to allow mixing to occur post-atmospheric discharge thereby reducing the pressure

drop through the plenum space. In this scheme, the cooling tower plume assumes a coaxial structure with less humid air shielding the more humid air in the plume core. Plume abatement can be a side effect of water conservation cooling towers, but not necessarily *vice versa*. Condensing module technology and thermosyphon systems are intended for water conservation by means of cooling the hot, moist air and collecting the condensed water.

The review of plume modeling is the more substantial contribution of this work; it starts with the classic Briggs' two-thirds law, then focuses on more advanced integral modeling. Several different entrainment assumptions are examined. The model of Schatzmann and Policastro [128] is described in detail as an example illustrating the formulation, capability and limitation of integral models. Plume-tower interactions can be accounted for empirically by adding a drag term, whereas the more complicated phenomenon of plume touchdown can be modeled only if detailed information of the tower wake is available. Several theoretical attempts to model plume merger yield good agreement with experimental data, however, these models are, by necessity, associated with restrictive assumptions e.g. of a still ambient/weak crossflow or strong crossflow, where the plume is respectively quasi-vertical or bent-over.

CFD simulations are able to describe some complex phenomena, such as recirculation, downwash, plume merger and drift deposition, however, this comes at an elevated computational cost. In the case of complex cooling tower structures or topography, similitude laboratory experiments seem to be equally promising. Wind tunnel, water tank and water flume experiments have been performed to account for different plume source and environmental conditions.

Several topics of greater complication are ambient turbulence, plume bifurcation and drift deposition. The effect of ambient turbulence has been incorporated by adding into previous integral models an extrainment velocity or terms related to second-order statistics. Some plausible hypotheses from potential flow theory have been made to describe the mechanism of bifurcation, however, no firm conclusion has been made regarding the conditions (e.g. buoyancy and ambient stratification) that define its onset. Finally, the drift deposition rate, its area of effect and the lifetime of emitted water droplets have all been predicted by using various CFD algorithms. These studies show that the same factors that aid in plume abatement e.g. a high ambient dry-bulb temperature are also conducive to reducing drift deposition.

This review can motivate future research in a number of different areas. In terms of plume abatement, the utility of the solar collectors can and should be further explored. For instance, the dry section e.g. depicted in Fig. 8 can be replaced by solar absorbing material through which the ambient air, to be mixed with the moist air from the cooling tower fill, is driven by the fan. Such a design is expected to reduce the capital cost, although the dry heating performance and, by extension, the dimension of solar absorber material must be tailored specifically to achieve plume abatement. Another idea is to extend the thermosyphon design in Mantelli [99] into hybrid cooling towers, possibly by locating the porous media structure in the plenum chamber. In these designs, a coaxial plume structure occurs above the cooling tower. The dynamics of coaxial plumes in a stratified ambient or a bounded environment merit further studies. There are also designs e.g. Libert et al. [92] that result in a plume source that is half wet and half dry. Plumes that are non-uniform at the source are yet to be fully understood. In a similar spirit, the buoyancy flux of a cooling tower plume may vary according to the time-dependent cooling demand of the power plant; the behavior (rise height and dilution) of such an unsteady source plume in a crosswind has not been thoroughly studied. In terms of plume merger, a generalized model is yet

to be proposed. Such a merger model should accommodate an arbitrary number of plume sources subject to arbitrary wind speed and direction.

Acknowledgements Financial support was generously provided by Natural Sciences and Engineering Research of Canada (NSERC) (Grant No. NSERC CRDJ 501081-16.), International Cooling Tower Inc. and the China Scholarship Council (CSC).

References

1. Abdelwahed MS, Chu VH (1978) Bifurcation of buoyant jets in a crossflow. In: Verification of mathematical and physical models in hydraulic engineering. ASCE, pp 819–826
2. Abraham G (1970) Round buoyant jet in cross-flow. In: 5th Internotional conf. water pollut. res. San Francisco, USA
3. Alton B, Davidson G, Slawson P (1993) Comparison of measurements and integral model predictions of hot water plume behaviour in a crossflow. Atmos Environ Part A Gen Top 27(4):589–598
4. Andersson B, Andersson R, Håkansson L, Mortensen M, Sudiyo R, Van Wachem B (2011) Computational fluid dynamics for engineers. Cambridge University Press, Cambridge
5. Andreopoulos J (1989a) Wind tunnel experiments on cooling tower plumes: part I—in uniform crossflow. J Heat Transfer 111(4):941–948
6. Andreopoulous J (1989b) Wind tunnel experiments on cooling tower plumes: Part II - in nonuniform cross flow of boundary layer type. NASA STI/Recon Technical Report N 111(4):949–955
7. Anfossi D, Bonino G, Bossa F (1967) Richiardone R (1978) Plume rise from multiple sources: a new model. Atmos Environ 12(9):1821–1826
8. Arakeri JH, Das D, Srinivasan J (2000) Bifurcation in a buoyant horizontal laminar jet. J Fluid Mech 412:61–73
9. Atc C (2011) Acceptance test procedure for wet-dry plume abatement cooling towers. Cooling Tower Institute, Houston
10. Baines W, Turner J (1969) Turbulent buoyant convection from a source in a confined region. J Fluid Mech 37(1):51–80
11. Baines WD (1983) A technique for the direct measurement of volume flux of a plume. J Fluid Mech 132:247–256
12. Becker B, Stewart W, Walter T, Becker C (1989) A numerical model of cooling tower plume recirculation. Math Comput Modell 12(7):799–819
13. Bennett M, Sutton S, Gardiner D (1992) Measurements of wind speed and plume rise with a rapid-scanning lidar. Atmos Environ Part A Gen Top 26(9):1675–1688
14. Bornoff R, Mokhtarzadeh-Dehghan M (2001) A numerical study of interacting buoyant cooling-tower plumes. Atmos Environ 35(3):589–598
15. Briggs GA (1969) Plume rise usaec critical review series tid-25075. Virginia, National Technical Information Service, Springfield, p 22161
16. Briggs GA (1975) Plume rise predictions. Lectures on air pollution and environmental impact analyses. American Meteorological Society, Boston, pp 59–111
17. Briggs GA (1984) Plume rise and buoyancy effects. Atmos Sci Power Prod 850
18. Brown G, Fletcher D (2005) CFD prediction of odour dispersion and plume visibility for alumina refinery calciner stacks. Process Saf Environ Prot 83(3):231
19. Bugler T, Lane J, Fields B, Miller RD (2010) Cooling towers, drift and legionellosis. J Cool Tower Inst 31(1):30–47
20. Canepa E (2004) An overview about the study of downwash effects on dispersion of airborne pollutants. Environ Model Softw 19(12):1077–1087

21. Carbonaro MG (1983) Air channeling device for mixing dry and humid air streams of a combined wet and dry atmospheric cooler. US Patent 4,367,183
22. Carhart R, Policastro A (1991) A second-generation model for cooling tower plume rise and dispersion–i single sources. Atmos Environ Part A Gen Top 25(8):1559–1576
23. Cenedese C, Linden PF (2014) Entrainment in two coalescing axisymmetric turbulent plumes. J Fluid Mech 752
24. Chahine A, Matharan P, Wendum D, Musson-Genon L, Bresson R, Carissimo B (2015) Modelling atmospheric effects on performance and plume dispersal from natural draft wet cooling towers. J Wind Eng Ind Aerodyn 136:151–164
25. Chen NC (1977) Review of cooling tower drift deposition models. Tech. rep., Oak Ridge National Lab., TN (USA)
26. Cintolesi C, Petronio A, Armenio V (2018) Turbulent structures of buoyant jet in cross-flow studied through large-eddy simulation. Environ Fluid Mech pp 1–33
27. Cizek J, Nozicka J (2016) Cooling tower plume. In: AIP conference proceedings, AIP Publishing, vol 1768, p 020001
28. Consuegro A, Kaiser A, Zamora B, Sánchez F, Lucas M, Hernández M (2014) Numerical modeling of the drift and deposition of droplets emitted by mechanical cooling towers on buildings and its experimental validation. Build Environ 78:53–67
29. Contini D, Robins A (2001) Water tank measurements of buoyant plume rise and structure in neutral crossflows. Atmos Environ 35(35):6105–6115
30. Contini D, Robins A (2004) Experiments on the rise and mixing in neutral crossflow of plumes from two identical sources for different wind directions. Atmos Environ 38(22):3573–3583
31. Contini D, Hayden P, Robins A (2006) Concentration field and turbulent fluxes during the mixing of two buoyant plumes. Atmos Environ 40(40):7842–7857
32. Contini D, Donateo A, Cesari D, Robins A (2011) Comparison of plume rise models against water tank experimental data for neutral and stable crossflows. J Wind Eng Ind Aerodyn 99(5):539–553
33. Contini D, Robins A, Hayden P (2014) Statistical properties of concentration fluctuations in two merging plumes. Environ Fluid Mech 14(4):919–942
34. Csanady G (1971) Bent-over vapor plumes. J Appl Meteorol 10(1):36–42
35. Davidson G (1982) Source flux corrections in analytical vapor plume models. J Appl Meteorol 21(12):1792–1797
36. Davidson G (1986) A discussion of Schatzmann's integral plume model from a control volume viewpoint. J Clim Appl Meteorol 25(6):858–867
37. Davidson G (1967) (1989) Simultaneous trajectory and dilution predictions from a simple integral plume model. Atmos Environ 23(2):341–349
38. Davis L, Shirazi M, Siegel D (1978) Measurement of buoyant jet entrainment from single and multiple sources. J Heat Transf 100(3):442–447
39. Demuren AO, Rodi W (1987) Three-dimensional numerical calculations of flow and plume spreading past cooling towers. J Heat Transf 109(1):113–119
40. Devenish B, Rooney G, Webster H, Thomson D (2010) The entrainment rate for buoyant plumes in a crossflow. Bound-Layer Meteorol 134(3):411–439
41. Djurfors S (1977) On the rise of buoyant plumes in turbulent environments. Professional Paper 1977-4, Syncrude Canada Ltd
42. Ernst GG, Davis JP, Sparks RSJ (1994) Bifurcation of volcanic plumes in a crosswind. Bull Volcanol 56(3):159–169
43. Fanaki F (1975) Experimental observations of a bifurcated buoyant plume. Bound-Layer Meteorol 9(4):479–495
44. Fernandes JH (1979) Vortex cooling tower. US Patent 4,157,368
45. Gangoiti G, Sancho J, Ibarra G, Alonso L, Garcia J, Navazo M, Durana N, Ilardia J (1997) Rise of moist plumes from tall stacks in turbulent and stratified atmospheres. Atmos Environ 31(2):253–269
46. Ge G, Xiao F, Wang S, Pu L (2012) Effects of discharge recirculation in cooling towers on energy efficiency and visible plume potential of chilling plants. Appl Therm Eng 39:37–44
47. Golay M, Glantschnig W (1967) Best F (1986) Comparison of methods for measurement of cooling tower drift. Atmos Environ 20(2):269–291
48. Golubovic MN, Hettiarachchi HM, Worek WM (2007) Evaluation of rotary dehumidifier performance with and without heated purge. Int Commun Heat Mass Transf 34(7):785–795
49. Guo DP, Yao RT, Fan D (2014) Wind tunnel experiment for predicting a visible plume region from a nuclear power plant cooling tower. J Appl Meteorol Climatol 53(2):234–241
50. Hamza R, Golay M (1981) Behavior of buoyant moist plumes in turbulent atmospheres. [Cambridge, Mass.]: Massachusetts Institute of Technology, Energy Laboratory

51. Hargreaves DM, Scase MM, Evans I (2012) A simplified computational analysis of turbulent plumes and jets. Environ Fluid Mech 12(6):555–578
52. Hayashi T (1971) Turbulent buoyant jets of effluent discharged vertically upwards from an orifice in a cross-current in the ocean. In: Proc. 14th congress, Int. Assoc. Hydr. Res., Paris, Aug, pp 157–165
53. Hensley JC (2009) Cooling tower fundamentals. Compiled from the knowledge and experience of the entire SPX cooling technologies staff. SPX cooling technologies. Inc Overland Park, Kansas USA
54. Holiday RA, Alsayed S (2015) Sustainability in cooling system operation. J Cooling Tower Inst 36(1):74–78
55. Hoult DP, Weil JC (1972) Turbulent plume in a laminar cross flow. Atmos Environ (1967) 6(8):513–531
56. Hoult DP, Fay JA, Forney LJ (1969) A theory of plume rise compared with field observations. J Air Pollut Control Assoc 19(8):585–590
57. Houx Jr JR, Landon RD, Lindahl Jr PA (1978) Bottom vented wet-dry water cooling tower. US Patent 4,076,771
58. Hubbard BJ, Mockry EF, Kinney Jr O (2003) Air-to-air atmospheric exchanger for condensing cooling tower effluent. US Patent 6,663,694
59. Hübner J (2004) Buoyant plumes in a turbulent environment. Ph.D. thesis, University of Cambridge
60. Hunt G, Kaye N (2005) Lazy plumes. J Fluid Mech 533:329–338
61. Huq P, Dhanak M (1996) The bifurcation of circular jets in crossflow. Phys Fluids 8(3):754–763
62. Huq P, Stewart E (1996) A laboratory study of buoyant plumes in laminar and turbulent crossflows. Atmos Environ 30(7):1125–1135
63. Jaber H, Webb R (1989) Design of cooling towers by the effectiveness-ntu method. J Heat Transf 111(4):837–843
64. Janicke U, Janicke L (2001) A three-dimensional plume rise model for dry and wet plumes. Atmos Environ 35(5):877–890
65. Jirka GH (2004) Integral model for turbulent buoyant jets in unbounded stratified flows. Part I: single round jet. Environ Fluid Mech 4(1):1–56
66. Jirka GH (2006) Integral model for turbulent buoyant jets in unbounded stratified flows Part II: Plane jet dynamics resulting from multiport diffuser jets. Environ Fluid Mech 6(1):43–100
67. Jirka GH, Fong HL (1981) Vortex dynamics and bifurcation of buoyant jets in crossflow. J Am Soc Civ Eng 107:479–499
68. Kaye N, Linden P (2004) Coalescing axisymmetric turbulent plumes. J Fluid Mech 502:41–63
69. Kaye N, Flynn M, Cook MJ, Ji Y (2010) The role of diffusion on the interface thickness in a ventilated filling box. J Fluid Mech 652:195–205
70. Khandekar M, Murty T (1975) A note on bifurcation of buoyant bent-over chimney plumes (1967). Atmos Environ 9(8):759–762
71. Kinney Jr OL, Brenneke GS, Bugler III TW (1999) Dry-air-surface heat exchanger. US Patent 5,944,094
72. Klimanek A (2013) Numerical modelling of natural draft wet-cooling towers. Arch Comput Methods Eng 20(1):61–109
73. Klimanek A, Białecki R (2009) Solution of heat and mass transfer in counterflow wet-cooling tower fills. Int Commun Heat Mass Transf 36(6):547–553
74. Klimanek A, Białecki RA, Ostrowski Z (2010) CFD two-scale model of a wet natural draft cooling tower. Numer Heat Transf Part A Appl 57(2):119–137
75. Klimanek A, Cedzich M, Białecki R (2015) 3D CFD modeling of natural draft wet-cooling tower with flue gas injection. Appl Therm Eng 91:824–833
76. Kloppers JC, Kröger DG (2005a) Cooling tower performance evaluation: Merkel, poppe, and e-ntu methods of analysis. J Eng Gas Turbines Power 127(1):1–7
77. Kloppers JC, Kröger DG (2005b) A critical investigation into the heat and mass transfer analysis of counterflow wet-cooling towers. Int J Heat Mass Transf 48(3–4):765–777
78. König C, Mokhtarzadeh-Dehghan M (2002) Numerical study of buoyant plumes from a multi-flue chimney released into an atmospheric boundary layer. Atmos Environ 36(24):3951–3962
79. Koo JB (2016a) Plume abatement cooling tower. KR Patent 20160007843
80. Koo JB (2016b) Plume abatement cooling tower. KR Patent 20160109975
81. Kröger DG (2004) Air-cooled heat exchangers and cooling towers, vol 1. PennWell Books
82. Kundu PK (1990) Fluid mechanics, 1st edn. Academic Press, San Diego
83. Lai AC, Lee JH (2012) Dynamic interaction of multiple buoyant jets. J Fluid Mech 708:539–575
84. Lai AC, Law AWK, Adams EE (2019) A second-order integral model for buoyant jets with background homogeneous and isotropic turbulence. J Fluid Mech 871:271–304

85. Latimer D, Samuelsen G (1978) Visual impact of plumes from power plants: a theoretical model. Atmos Environ (1967) 12(6–7):1455–1465
86. Laulainen N, Webb R, Wilber K, Ulanski S (1979) Comprehensive study of drift from mechanical draft cooling towers. Final report. Tech. rep., Battelle Pacific Northwest Labs., Richland, WA (USA)
87. Launder B, Spalding D (1974) The numerical computation of turbulent flows. Comput Methods Appl Mech Eng 3(2):269–289
88. Lavelle J (1997) Buoyancy-driven plumes in rotating, stratified cross flows: plume dependence on rotation, turbulent mixing, and cross-flow strength. J Geophys Res Oceans 102(C2):3405–3420
89. Lee J (2018) Evaluation of impacts of cooling tower design properties on the near-field environment. Nucl Eng Des 326:65–78
90. Li S, Flynn M (2020) Merging of two plumes from area sources with applications to cooling towers. Phys Rev Fluids (submitted)
91. Li S, Moradi A, Vickers B, Flynn M (2018) Cooling tower plume abatement using a coaxial plume structure. Int J Heat Mass Transf 120:178–193
92. Libert JP, Hamilton J, Bugler T (2015) Advanced cooling solutions for water conservation. J Cool Tower Inst 36(1):66–72
93. Lindahl P, Jameson RW (1993) Plume abatement and water conservation with the wet/dry cooling tower. Tech. rep., Electric Power Research Inst., Palo Alto, CA (United States); Yankee Scientific, Inc., Medfield, MA (United States)
94. Lindahl P, Mortensen K (2010) Plume abatement-the next generation. J Cool Tower Inst 31(2):8–24
95. List E (1982) Turbulent buoyant jets and plumes: HMT: the science & applications of heat and mass transfer. Reports, Reviews & Computer Programs, vol 6. Elsevier
96. Liu Z, Bao B (2014) Research on reducing recirculation influence of warm and saturated air discharged from cooling towers. J Cool Tower Inst 35(1):48–56
97. Lucas M, Martinez PJ, Ruiz J, Kaiser AS, Viedma A (2010) On the influence of psychrometric ambient conditions on cooling tower drift deposition. Int J Heat Mass Transf 53(4):594–604
98. Macdonald R, Strom R, Slawson P (2002) Water flume study of the enhancement of buoyant rise in pairs of merging plumes. Atmos Environ 36(29):4603–4615
99. Mantelli MH (2016) Development of porous media thermosyphon technology for vapor recovering in cross-current cooling towers. Appl Therm Eng 108:398–413
100. Merkel F (1925) Verdunstungskühlung. VDI-Verlag
101. Meroney RN (2006) CFD prediction of cooling tower drift. J Wind Eng Ind Aerodyn 94(6):463–490
102. Meroney RN (2008) Protocol for CFD prediction of cooling-tower drift in an urban environment. J Wind Eng Ind Aerodyn 96(10–11):1789–1804
103. Meyer J (1974) Mechanical-draft cooling tower visible plume behavior: measurements, models, prediction. Cool Tower Environ pp 307–352
104. Michioka T, Sato A, Kanzaki T, Sada K (2007) Wind tunnel experiment for predicting a visible plume region from a wet cooling tower. J Wind Eng Ind Aerodyn 95(8):741–754
105. Mokhtarzadeh-Dehghan M, König C, Robins A (2006) Numerical study of single and two interacting turbulent plumes in atmospheric cross flow. Atmos Environ 40(21):3909–3923
106. Monjoie M, Libert JP (1994) Testing procedures for wet/dry plume abatement cooling towers. CTI J 15:56
107. Moon JS (2017) Vortex—cooling tower having an air mixer. KR Patent 101724128(B1)
108. Mortensen K (2009) Use of Air2Air technology to recover fresh-water from the normal evaporative cooling loss at coal-based thermoelectric power plants. Tech. rep, SPX Cooling Technologies Incorporated
109. Morton B (1957) Buoyant plumes in a moist atmosphere. J Fluid Mech 2(02):127–144
110. Morton B, Taylor G, Turner J (1956) Turbulent gravitational convection from maintained and instantaneous sources. Proc R Soc Lond A Math Phys Eng Sci R Soc 234:1–23
111. Murphy B (1975) Plume rise from a row of chimneys. In: 68th Annual meeting of the Air Pollution Control Association, Paper No, pp 75–04
112. Netterville DD (1990) Plume rise, entrainment and dispersion in turbulent winds. Atmos Environ Part A Gen Top 24(5):1061–1081
113. Ooms G, Mahieu A (1981) A comparison between a plume path model and a virtual point source model for a stack plume. Appl Sci Res 36(5–6):339–356
114. Palmer B (2006) Method and system for recovering vapor exhaust from processing equipment. US Patent App. 11/523,318
115. Policastro A, Wastag M (1981) Studies on mathematical models for characterizing plume and drift behavior from cooling towers. Volume 1. Review of european research. Tech. rep., Argonne National Lab., IL (USA)

116. Poppe M, Rögener H (1991) Berechnung von rückkühlwerken. VDI Wärmeatlas, pp Mi
117. Priestley C (1953) Buoyant motion in a turbulent environment. Aust J Phys 6(3):279–290
118. Priestley C, Ball F (1955) Continuous convection from an isolated source of heat. Q J R Meteorol Soc 81(348):144–157
119. Roffman A, Van Vleck LD (1974) The state-of-the-art of measuring and predicting cooling tower drift and its deposition. J Air Pollut Control Assoc 24(9):855–859
120. Rooney GG (2015) Merging of a row of plumes or jets with an application to plume rise in a channel. J Fluid Mech 771
121. Rooney GG (2016) Merging of two or more plumes arranged around a circle. J Fluid Mech 796:712–731
122. Rouse H, Yih CS, Humphreys H (1952) Gravitational convection from a boundary source. Tellus 4(3):201–210
123. Ruscheweyh H (1984) A mixing system for gas flow. J Wind Eng Ind Aerodyn 16(2–3):189–199
124. Ruscheweyh H (1985) Apparatus for uniformizing the parameters of a flow and/or for mixing together at least two individual streams which discharge into a main flow. US Patent 4,527,903
125. Sánchez F, Kaiser A, Zamora B, Ruiz J, Lucas M (2015) Prediction of the lifetime of droplets emitted from mechanical cooling towers by numerical investigation. Int J Heat Mass Transf 89:1190–1206
126. Schatzmann M (1978) The integral equations for round buoyant jets in stratified flows. Zeitschrift für angewandte Mathematik und Physik ZAMP 29(4):608–630
127. Schatzmann M (1979) An integral model of plume rise. Atmos Environ (1967) 13(5):721–731
128. Schatzmann M, Policastro AJ (1984) An advanced integral model for cooling tower plume dispersion. Atmos Environ (1967) 18(4):663–674
129. Schulze HD (2010) Hybrid cooling tower. EP2141429 (A2)
130. Scorer RS (1958) Natural aerodynamics. Pergamon, London
131. Scorer RS (1968) Air Pollution. Pergamon Press, Oxford
132. Shih TH, Liou WW, Shabbir A, Yang Z, Zhu J (1995) A new k-ϵ eddy viscosity model for high Reynolds number turbulent flows. Comput Fluids 24(3):227–238
133. Slawson P, Csanady G (1967) On the mean path of buoyant, bent-over chimney plumes. J Fluid Mech 28(2):311–322
134. Slawson P, Csanady G (1971) The effect of atmospheric conditions on plume rise. J Fluid Mech 47(1):33–49
135. Streng A (1998) Combined wet/dry cooling towers of cell-type construction. J Energy Eng 124(3):104–121
136. Takata K, Nasu K, Yoshikawa H (1996) Prediction of the visible plume from a cooling tower. Cooling Tower Institute
137. Takata K, Michioka T, Kurose R (2016) Prediction of a visible plume from a dry and wet combined cooling tower and its mechanism of abatement. Atmosphere 7(4):59
138. Talbot JJ (1979) A review of potential biological impacts of cooling tower salt drift. Atmos Environ (1967) 13(3):395–405
139. Taylor GI (1945) Dynamics of a mass of hot gas rising in air. U.S. Atomic Energy Commission MDDC 919. LADC 276
140. Teixeira MA, Miranda PM (1996) On the entrainment assumption in Schatzmann's integral plume model. Appl Sci Res 57(1):15–42
141. Tohidi A, Kaye NB (2016) Highly buoyant bent-over plumes in a boundary layer. Atmos Environ 131:97–114
142. Turner J (1960) A comparison between buoyant vortex rings and vortex pairs. J Fluid Mech 7(3):419–432
143. Turner J (1963) The motion of buoyant elements in turbulent surroundings. J Fluid Mech 16(1):1–16
144. Tyagi S, Wang S, Ma Z (2007) Prediction, potential and control of plume from wet cooling tower of commercial buildings in Hong Kong: a case study. Int J Energy Res 31(8):778–795
145. Veldhuizen H, Ledbetter J (1971) Cooling tower fog: control and abatement. J Air Pollut Control Assoc 21(1):21–24
146. Waitz I, Qiu Y, Manning T, Fung A, Elliot J, Kerwin J, Krasnodebski J, O'Sullivan M, Tew D, Greitzer E et al (1997) Enhanced mixing with streamwise vorticity. Prog Aerosp Sci 33(5–6):323–351
147. Walser SM, Gerstner DG, Brenner B, Höller C, Liebl B, Herr CE (2014) Assessing the environmental health relevance of cooling towers-a systematic review of legionellosis outbreaks. Int J Hyg Environ Health 217(2–3):145–154
148. Wang J, Wang S, Xu X, Xiao F (2009) Evaluation of alternative arrangements of a heat pump system for plume abatement in a large-scale chiller plant in a subtropical region. Energy Build 41(6):596–606

149. Wang S, Tyagi S (2006) Report on the prediction, potential and control of plume from cooling towers of international commerce center. The Hong Kong Polytechnic University, Hong Kong
150. Wang S, Tyagi S, Sharma A, Kaushik S (2007) Application of solar collectors to control the visible plume from wet cooling towers of a commercial building in Hong Kong: a case study. Appl Therm Eng 27(8):1394–1404
151. Wang W, Ge X, Zhao S, Zheng H, Xu W, Lv J, Zhu G (2019) A novel approach for water conservation and plume abatement in mechanical draft cooling towers. Atmosphere 10(12):734
152. Wigley T (1975) Condensation in jets, industrial plumes and cooling tower plumes. J Appl Meteorol 14(1):78–86
153. Wigley T, Slawson P (1971) On the condensation of buoyant, moist, bent-over plumes. J Appl Meteorol 10(2):253–259
154. Wigley T, Slawson P (1972) A comparison of wet and dry bent-over plumes. J Appl Meteorol 11(2):335–340
155. Winiarski LD, Frick WF (1976) Cooling tower plume model. US Environmental Protection Agency, Office of Research and Development
156. Winter A (1997) Control of visible plumes from cooling towers. Proc Inst Mech Eng Part A J Power Energy 211(1):67–72
157. Witham F, Phillips JC (2008) The dynamics and mixing of turbulent plumes in a turbulently convecting environment. J Fluid Mech 602:39–61
158. Wooler P, Burghart G, Gallagher J (1967) Pressure distribution on a rectangular wing with a jet exhausting normally into an airstream. J Aircr 4(6):537–543
159. Wu FH, Koh RC (1978) Mathematical model for multiple cooling tower plumes, vol 1. US Environmental Protection Agency, Office of Research and Development, Environmental Research Laboratory
160. Yakhot V, Orszag S, Thangam S, Gatski T, Speziale C (1992) Development of turbulence models for shear flows by a double expansion technique. Phys Fluids A 4(7):1510–1520
161. Zandian A, Ashjaee M (2013) The thermal efficiency improvement of a steam Rankine cycle by innovative design of a hybrid cooling tower and a solar chimney concept. Renew Energy 51:465–473